

## Thermal Stability of Self-Assembled Monolayers of *n*-hexanethiol on Au(111)-(1 × 1) and Au(001)-(1 × 1)

Lucila Josefina Cristina, Gustavo Ruano, Roberto C. Salvarezza, and Julio Ferron

*J. Phys. Chem. C*, **Just Accepted Manuscript** • DOI: 10.1021/acs.jpcc.7b05883 • Publication Date (Web): 20 Nov 2017

Downloaded from <http://pubs.acs.org> on December 1, 2017

### Just Accepted

“Just Accepted” manuscripts have been peer-reviewed and accepted for publication. They are posted online prior to technical editing, formatting for publication and author proofing. The American Chemical Society provides “Just Accepted” as a free service to the research community to expedite the dissemination of scientific material as soon as possible after acceptance. “Just Accepted” manuscripts appear in full in PDF format accompanied by an HTML abstract. “Just Accepted” manuscripts have been fully peer reviewed, but should not be considered the official version of record. They are accessible to all readers and citable by the Digital Object Identifier (DOI®). “Just Accepted” is an optional service offered to authors. Therefore, the “Just Accepted” Web site may not include all articles that will be published in the journal. After a manuscript is technically edited and formatted, it will be removed from the “Just Accepted” Web site and published as an ASAP article. Note that technical editing may introduce minor changes to the manuscript text and/or graphics which could affect content, and all legal disclaimers and ethical guidelines that apply to the journal pertain. ACS cannot be held responsible for errors or consequences arising from the use of information contained in these “Just Accepted” manuscripts.



1  
2  
3  
4 **Thermal Stability of Self-Assembled Monolayers of *n*-hexanethiol on**  
5  
6 **Au(111)-(1 × 1) and Au(001)-(1 × 1)**  
7  
8

9  
10  
11 **Lucila J. Cristina<sup>1\*</sup>, Gustavo Ruano<sup>1\*</sup>, Roberto Salvarezza<sup>2</sup> and Julio Ferrón<sup>1,3</sup>.**  
12  
13

14  
15  
16  
17  
18 <sup>1</sup> Instituto de Física del Litoral (IFIS Litoral), Universidad Nacional del Litoral - CONICET  
19 Gral. Güemes 3450, S3000GLN Santa Fe, Argentina.  
20

21  
22 <sup>2</sup> Instituto de Investigaciones Fisicoquímicas Teóricas y Aplicadas (INIFTA), Facultad de  
23 Ciencias Exactas, Universidad Nacional de La Plata - CONICET- Sucursal, 4 Casilla de  
24 Correo 16, (1900) La Plata, Argentina.  
25  
26

27  
28 <sup>3</sup> Departamento de Materiales. Facultad de Ingeniería Química. Universidad Nacional del  
29 Litoral. Santa Fe, Argentina.  
30  
31

32  
33  
34 \* Corresponding author  
35

36 Email: [lucila.cristina@santafe-conicet.gov.ar](mailto:lucila.cristina@santafe-conicet.gov.ar) , [gustavo.ruano@santafe-conicet.gov.ar](mailto:gustavo.ruano@santafe-conicet.gov.ar)  
37  
38  
39  
40  
41  
42  
43  
44  
45  
46  
47  
48  
49  
50  
51  
52  
53  
54  
55  
56  
57  
58  
59  
60

**Abstract**

The thermal desorption in ultra-high vacuum of *n*-hexanethiol (C6T) self-assembled monolayers (SAMs) prepared from ethanolic solutions on Au(111) and Au(001) unreconstructed surfaces was investigated by X-ray photoelectron spectroscopy. The SAMs desorption was performed from room temperature (RT) to 380 K. We reported that the hexanethiolate surface saturation coverage is bigger (~ 0.4 ML) for the SAM on Au(001) than on Au(111) (~ 0.33 ML). We identified a greater stability for C6T SAMs on Au(001). Large amounts of physisorbed species was found on preferred oriented (111) polycrystalline Au at the low coverage regime at RT, while the SAM on the Au(001) single-crystal at this conditions desorbs at a steady pace. At 340 K, both SAMs remain stable at the coverage expected for the lying-down phases that maximizes the van der Waals interactions. We observed that at higher temperatures the carbon alpha-sulfur bond cleavages producing free S on both gold surfaces.

## 1. Introduction

Self-assembled monolayers (SAMs) of thiols molecules (R-SH) on solid surfaces<sup>1-3</sup> are currently a hot topic due to the possibility of tuning the chemical identity of their surfaces. The fields of applications cover their use in the fabrication of organic and biomolecular electric nanoscale devices,<sup>4-6</sup> biosensors, catalysts, with applications in medicine and biochemistry,<sup>1,2,7</sup> among the most important ones. Growing thiol SAMs has become the most simple and efficient way for the functionalization of solid surfaces of noble metals, semiconductors and oxides with different substrate topographies: nanoparticles (NPs), single and poly crystals.<sup>1,8</sup> Due to its large chemical stability, interesting optical properties and biocompatibility, gold represents a natural choice for SAMs support material, and it has been used in many technological applications in this field.<sup>1</sup>

Thermal stability of thiol SAMs is of crucial importance in scaling these devices out of the laboratory to real life technological applications. In the development of SAMs-based devices, in which thermal and temporal stability is desirable, understanding the thermal stability and desorption mechanisms of organic monolayers on solid surfaces is one of the most important issues. Although the thermal stability and desorption processes of thiol SAMs on metal surfaces have been investigated at the molecular level with various techniques,<sup>9-16</sup> this point deserves indeed further investigation.

Because of the importance that nanotechnologies have reached in different fields, going from electronics to medicine, the growth of thiol SAMs on Au nanoparticles (AuNPs) has gained enormous attention in the last times.<sup>1,17-20</sup> The AuNPs present faceted monocrystalline (*fcc*) shapes, such as truncated octahedra and cuboctahedra, dominated by {111} and {100} facets.<sup>21-24</sup> The relative proportion of each of these crystallographic faces in AuNPs depends on their size and thermodynamic conditions. For instance, the surfaces of AuNPs of size greater than 3 nm exhibit approximately 30% of {100} faces, whereas the remaining 70% consisting of {111} planes.<sup>25</sup> The coexistence of these two faces in the same nanoparticle points out to the importance of studying the thiol self-assembly on both planar gold surfaces.

Due to its larger stability, most of the studies concerning thiol-based SAMs with aliphatic backbones adsorbed on gold planar surfaces have been performed on (111) Au

1  
2  
3 face.<sup>1,3,4,26</sup> The knowledge about this system is then clearly larger than over the (001) gold  
4 face. However, although some mechanisms are almost universally accepted, others are still  
5 matter of discussion. Temperature Programmed Desorption (TPD)<sup>10,11,13,15,27-31</sup> and  
6 Scanning Tunnelling Microscopy (STM)<sup>5,12,15,32-38</sup> have been extensively used to examine  
7 the interactions between thiols molecules chemisorbed on gold surfaces as well also  
8 intermolecular interactions under heat treatment. Thus, *n*-alkanethiols SAMs on Au(111)  
9 exhibit a desorption process of two-step. TPD measurements have shown that two  
10 neighboring monomers of alkanethiol SAMs on gold surfaces (alkanethiolates, R-S-Au)  
11 mainly desorbs associatively as dimer molecules (dialkyl disulfides, R-S-S-R),<sup>11-</sup>  
12 <sup>13,15,16,29,36,39,40</sup> by sample heating at 350-450 K. But at higher temperatures (400-500 K),  
13 they can desorb molecularly as thiols monomers (R-SH) through breaking of S–Au  
14 bonds.<sup>6,13-16,29,40</sup> Final desorption of a significant amount of RS–Au<sub>ad</sub> complexes is  
15 observed at around 700 K. Following total thiol SAM desorption, only little quantity of  
16 sulfur is detected indicating that S–C bond breaking. These S atoms on the Au(111) surface  
17 are difficult to remove even at high temperatures.<sup>41</sup> There are several factors governing the  
18 desorption processes. They are the molecular density, the molecular structure,<sup>11,29</sup> packing  
19 and orientation,<sup>15,40</sup> surface roughness,<sup>41</sup> substrate temperature in adsorption,<sup>10</sup> structure of  
20 thiol molecule,<sup>39</sup> and chain length alkanethiols,<sup>11</sup> among the most importants. Thus, for  
21 instance, while short chain alkanethiols molecules in a densely-packed phase (high  
22 coverage) desorb as disulfide molecules by heating the sample,<sup>29,39</sup> desorption mainly  
23 occurs through thiolate radicals release when they are present with a lower molecular  
24 density.<sup>10,39</sup>  
25  
26  
27  
28  
29  
30  
31  
32  
33  
34  
35  
36  
37  
38  
39  
40  
41  
42

43 Although a lot work on the subject has been performed in the last time, most of  
44 them over the (111) face of gold, many questions remains open, mainly concerning the  
45 (001) face. For instance, it has been suggested that thermal stability of SAMs on gold  
46 surface is limited to approximately 400 K,<sup>29,36</sup> and heat treatment has been employed to the  
47 construction of structures with large ordered domains and complex phase, using thermal  
48 diffusion of thiolate-gold complexes under vacuum conditions.<sup>35,42-44</sup> On the other hand,  
49 recent work demonstrated that SAMs of hexanethiol molecules chemisorbed on Au(111)  
50 surfaces desorbs spontaneously in high vacuum (HV) conditions ( $3 \times 10^{-7}$  Pa) at room  
51  
52  
53  
54  
55  
56  
57  
58  
59  
60

1  
2  
3 temperature (RT) and that van der Waals interactions play an important role in determining  
4 their structural stability.<sup>37</sup>  
5  
6

7  
8 In contrast to the extensive study on thermal desorption of SAMs of aliphatic thiol  
9 molecules on Au(111) surfaces, much less information can be found for such processes on  
10 Au(001) surfaces. It has been reported that physisorbed butanethiol on Au(001)-(5×20)  
11 desorbs molecularly at ~138 K using TPD. On the other hand, desorption of the  
12 chemisorbed butanethiolate is accompanied by decomposition to yield primarily 1-butene at  
13 ~500 K; the thiol sulfur remains adsorbed on the (100) surface and either desorbs or  
14 possibly dissolves into the bulk of the gold substrate at above 700 K.<sup>45</sup> STM topography of  
15 butanethiol SAM on Au(001) showed migration of surface Au atoms and the island phase  
16 coarsened driven by a reduction in the island edge energy after storage for two days in HV  
17 at RT.<sup>14</sup> The desorption data demonstrated that this self-assembled monolayer is thermally  
18 stable up to 373 K and desorbs molecularly above this temperature.  
19  
20  
21  
22  
23  
24  
25  
26

27  
28 In this paper, we report experiments performed to elucidate the mechanism  
29 associated with the desorption process of SAMs of hexanethiol molecules (C6T, C<sub>6</sub>H<sub>13</sub>SH)  
30 prepared by dipping in ethanolic solutions on two unreconstructed gold surfaces; the  
31 Au(111)-(1 × 1) and Au(001)-(1 × 1). We employed X-ray photoelectron spectroscopy  
32 (XPS) to follow the evolution of the different chemical species arising from the interaction  
33 alkanethiol-Au (i.e. thiolate, disulfide-free thiol, atomic sulfur). We obtained the relative  
34 amounts and coverage values of those species as a function of time for different values of  
35 temperature (i.e. room temperature, 340 K, 360 K and 380 K) in ultra-high vacuum (UHV).  
36  
37  
38  
39  
40  
41  
42  
43  
44

## 45 2. Experimental Methods

46  
47 **Gold Substrates.** The Au substrates used in this paper were single-crystals oriented better  
48 than 0.1 degree towards the (111)-face and (001)-face and top surface polished to a  
49 roughness < 0.03 μm of 10 mm in diameter (MaTeck). The Au(111)-(1 × 1) and Au(001)-  
50 (1 × 1) surfaces were prepared by butane flame annealing and cooled down at room  
51 temperature. We also used preferred oriented Au(111) substrates prepared by flame  
52 annealing of evaporated Au on chromium-coated glass plates (Arrandee<sup>TM</sup>) to study the role  
53 of substrate order on thermal desorption.  
54  
55  
56  
57  
58  
59  
60

1  
2  
3 **SAMs preparation.** We have used *n*-hexanethiol molecules (Sigma-Aldrich, 95%) as a test  
4 system. C6T self-assembled monolayers were prepared by immersing the freshly prepared  
5 substrates in 100  $\mu$ M C6T ethanolic solutions (BASF 99%) for 24 h at RT in absence of  
6 light. After the SAMs were formed, the Au substrates were removed from the solution and  
7 rinsed several times with plenty of ethanol and Milli-Q water to remove entrapped  
8 physisorbed species.<sup>46</sup> Finally, the samples were dried under a N<sub>2</sub> flow, mounted on a  
9 molybdenum sample holder for heating experiments, and transferred to the ultra-high  
10 vacuum chamber to perform the photoemission experiments. The typical time needed for  
11 transferring the sample from atmosphere to the UHV chamber, and performing the first ( $t_0$ )  
12 measurement, was less than 20 min.

13  
14  
15  
16  
17  
18  
19  
20  
21 **Thermal treatment.** Two types of desorption experiments were performed in the UHV  
22 chamber ( $P = 1 \times 10^{-10}$  mbar): 1) the SAMs/substrates XPS spectra were acquired at RT as a  
23 function of time (hours, days, weeks), and 2) the samples were heated at a fixed  
24 temperature in the range from 340 to 380 K during certain time (from 1 to several minutes).  
25 After this heating period, the samples were rapidly cooled down to RT and the XPS  
26 spectrum was taken in the same chamber. The temperature was monitored by a type K  
27 thermocouple located at the sample edge. As the desorption process destroy the C6T  
28 SAMs, a freshly prepared monolayer was used at each temperature (RT, 340 K etc.). This  
29 differs from the continuous temperature variation methods in TPD measurements in which  
30 the same thiol SAM is used in the whole temperature range. Additionally, each desorption  
31 experiment was performed at least in duplicate on both faces of the Au substrate.

32  
33  
34  
35  
36  
37  
38  
39  
40  
41 **XPS Measurements.** The photoemission experiments were carried out in a commercial  
42 surface analysis SPECS system, equipped with a hemispherical energy analyzer, a  
43 differentially-pumped mass analyzed ion gun, and a double anode X-ray source. The base  
44 pressure in the analyzer chamber was in the low  $10^{-10}$  mbar range. The XPS spectra were  
45 collected after exciting the sample with a no-monochromatized MgK $\alpha$  radiation at 1253.6  
46 eV, with a 150 mm hemispherical electron energy analyzer (SPECS Phoibos 150). The  
47 surface cleanliness was checked with survey XPS spectra in which only the characteristic  
48 signals of S, C and Au were detected. The high-resolution S 2p, C 1s, O 1s and Au 4f<sub>7/2</sub>  
49 core-level spectra were acquired using the fixed analyzer transmission (FAT) mode with  
50 analyzer pass energy of 10 eV and used as a proof of the SAM quality. The binding energy  
51  
52  
53  
54  
55  
56  
57  
58  
59  
60

(BE) scales for the C6T SAMs on Au surfaces were calibrated by setting the Au 4f<sub>7/2</sub> BE to 84.0 eV with respect to the Fermi level. The detailed S 2p spectra were fitted with a Shirley-type background and two elemental components 2p<sub>3/2</sub>-2p<sub>1/2</sub> doublets, each composed of two combinations of Lorentzian and Gaussian (Voigt) functions. The spin-orbit doublet separation of the S 2p signal was fixed to 1.18 eV and the intensity ratio to 2:1.<sup>47</sup> During the fittings, the positions, intensities, and Gaussian full widths at half-maximum (fwhm) of these components were modified to achieve the best adjustment; and the Lorentzian fwhm was fixed at 0.15 eV, as was done in previous work.<sup>48,49</sup>

The possibility of X-ray beam damage is an issue that deserves consideration.<sup>50,51</sup> In order to evaluate if the C6T films on gold undergoes any degradation process under X-ray bombardment, ten S 2p XPS spectra were acquired for each experimental point. Each of the 10 spectra was in turn the average of 5-10 scans, where each run was taken with 0.025 eV steps, holding for 0.1 s. Five Au 4f spectra of one scan were taken alternately. The full measurement process lasts around one hour, with the X-rays beam impinging on the same spot (all the sample). Since no differences were observed among any spectra, in particular between the first and the last one (one hour more irradiated), we are sure that no detectable damage was induced to the sample by the X-rays beam. After this process, we average all the spectra to improve the signal to noise ratio. It is to be noticed that all XPS measurements, including those corresponding to the high (340-380 K) temperature, were taken at RT where the thermal desorption occurring during one hour can be neglected.

### 3. Results and discussion

#### 3.1. SAMs coverage.

The formation, structure, and molecular packing of alkanethiol monolayers is driven by three different classes of interactions: *i*) between thiol head groups and Au substrate, *ii*) between alkanethiol end groups, and *iii*) van der Waals (vdW) forces between alkyl chains of neighboring molecules that stabilize the structure.<sup>4,2,52</sup> Thus, the aliphatic thiols molecules can both physisorb on Au surface through vdW interactions, which depends on the alkyl chain length, and chemisorb through the strong covalent thiolate bonds (R-S-Au). These interactions can be exposed by examining S 2p and Au 4f photoemission spectra.



1  
2  
3  
4  
5  
6  
7  
8  
9  
10  
11  
12  
13  
14  
15  
16  
17  
18  
19  
20  
21  
22  
23  
24  
25  
26  
27  
28  
29  
30  
31  
32  
33  
34  
35  
36  
37  
38  
39  
40  
41  
42  
43  
44  
45  
46  
47  
48  
49  
50  
51  
52  
53  
54  
55  
56  
57  
58  
59  
60

As a first step, we study the quality of hexanethiol self-assembled monolayers on both faces of gold single-crystals from liquid-phase adsorption, at saturation coverage ( $t_0$ ). The samples were introduced in the UHV chamber immediately after the immersion in the same ethanolic solution for 24 h to start the first ( $t_0$ ) measurement. In Figure 1, we show the S 2p XPS spectra for fully covered C6T SAMs on both unreconstructed surfaces: Au(111)-(1 × 1) (up) and Au(001)-(1 × 1) (down). Following the usual curve-fitting analysis, two different S states are necessary to explain the spectra. Regardless of the substrate, the S 2p core level signal was decomposed in two distinctive S components:  $S_A$  and  $S_B$ . Each of these S 2p components displays a S 2p<sub>3/2</sub> and S 2p<sub>1/2</sub> spin-orbital splitting doublet of 1.18 eV<sup>47</sup> with the expected intensity relation of 2:1. The intensities of the S 2p spectra were normalized using the total area of the Au 4f peak. In this work, we will always refer to the position in binding energy (BE) of the S 2p<sub>3/2</sub> peak respect to the Au 4f<sub>7/2</sub> BE at 84.0 eV.

The binding energy for the most prominent S 2p<sub>3/2</sub> peaks ( $S_B$ ) are ( $161.96 \pm 0.02$ ) eV for C6T SAMs on the Au(111) and ( $161.81 \pm 0.01$ ) eV for Au(001) surfaces. These states were assigned to sulfur chemisorbed on the gold surface in agreement with what is generally reported for molecular thiols chemisorbed on Au systems,<sup>53,54</sup> indicating the formation of a hexanethiolate bond with the surface Au atoms ( $S_{B(\text{thiolate})}$ ).<sup>46,55</sup> The low core level shift (CLS) difference between hexanethiolate adsorbed on both gold faces ( $0.15 \pm 0.02$ ) eV confirms our previous report.<sup>56</sup> This result, as previously stated, supports the idea that the chemistry determines the BE of the S 2p core level rather than adsorption surface sites. This doublet is frequently accompanied by an additional remaining sulfur component at ( $163.27 \pm 0.08$ ) eV (S 2p<sub>3/2</sub>), which is independent of the gold face. This component is characteristic of physisorbed species<sup>57,58</sup> ( $S_{A(\text{physisorbed})}$ ), i.e. free thiol molecules, disulfide and dialkylsulfide species,<sup>46,59,60</sup> where the S-S (or S-H) chemical bond is so strong that makes the surface characteristics irrelevant. Other point supporting the idea of assigning  $S_A$  species to unbound molecules is its dependence on the SAM preparation, i.e. the  $S_{A(\text{physisorbed})}$  component is larger for non-well rinsed substrates.<sup>46</sup> On the other hand, in a few cases the S 2p XPS region spectra was fitted with three components. The extra sulfur state, at average S 2p<sub>3/2</sub> BE value of ( $161.04 \pm 0.08$ ) eV, is associated with atomically adsorbed sulfur ( $S_{C(\text{sulfide})}$ ) on both Au(111)<sup>61</sup> and Au(001)<sup>62</sup> faces. This could result from SAM degradation or impurities present in thiols,<sup>63</sup> and often appears in alkanethiol

monolayer with low coverage or initial disordered phase.<sup>29,64,65</sup> We take advantage of this fact to check the quality of the C6T SAMs. A quantitative analysis of the results depicted in Figure 1 gives around 80% for the hexanethiolate species on both surfaces, showing that the C6T molecules chemisorb mostly on gold surfaces, independently of the crystal face.

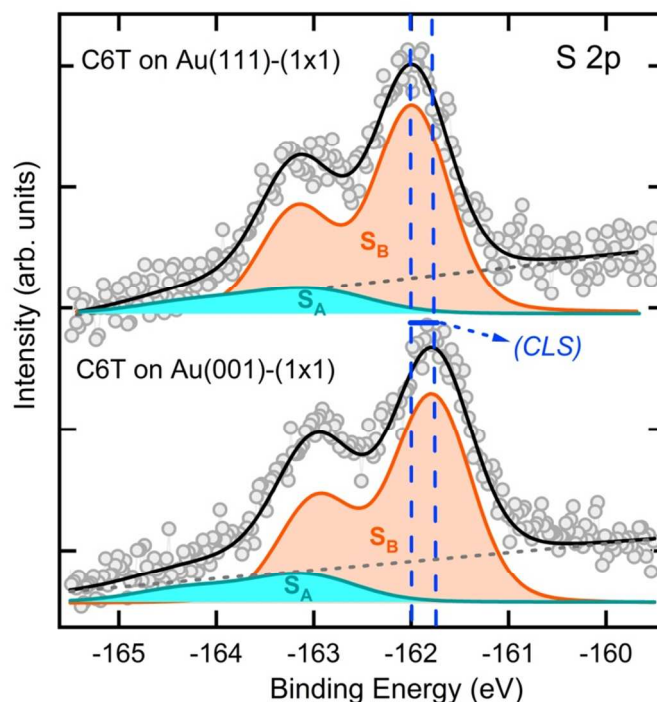


**Figure 1.** Comparison of S 2p XPS spectra for C6T SAMs on Au(111)-(1 × 1) and Au(001)-(1 × 1) obtained after a incubation of 24 h in a 100 μM ethanolic solution. Best fits (black line), S<sub>A</sub>: physisorbed molecules (free R-SH, disulfide (S–S bonds) or dialkyl sulfide species, S<sub>B</sub>: chemisorbed thiolate (R-S-Au bonds). The Core Level Shift (CLS) is shown in the figure.

The intensity of any core-level XPS peak is proportional to the number of atoms in the analysis volume. An estimation of the hexanethiolate surface saturation coverage ( $\theta_{\text{thiolate}}$ ) is obtained from the area ratio of the S 2p and Au 4f XPS peaks at  $t_0$ . In this work, the  $\theta_{\text{thiolate}}$  in the sample is defined as the ratio  $N_{\text{S}}^{\text{sup}}/N_{\text{Au}}^{(001)/(111)}$  between the surface density of thiol molecules and the density of surface Au atoms of the substrate on the face

(001) or (111), and can be written in terms of the intensity ratio of two peaks characteristic of each element as:

$$\frac{N_S^{sup}}{N_{Au}^{(001)/(111)}} = \left( \frac{\frac{d\sigma(Au4f)}{d\Omega}}{\frac{d\sigma(S2p)}{d\Omega}} \right) \frac{\lambda \cos \theta}{d_{\perp}^{(001)/(111)}} \left( \frac{I_{S2p}}{I_{Au4f}} \right)$$

where  $\frac{d\sigma(Au4f)}{d\Omega}$  and  $\frac{d\sigma(S2p)}{d\Omega}$  are the differential photoemission cross section,  $\lambda$  is the electron mean free path within the material,  $\theta$  is the angle between the observation direction and the surface normal, and  $d_{\perp}^{(001)/(111)}$  is the distance between planes (001) or (111) of the gold single-crystal. Coverages are given in monolayers (ML), with 1 ML defined as a 1:1 ratio between the density of S atoms on the surface and that of Au at the outermost gold surface (considered in our case as unreconstructed (111) and (001) planes). The initial surface coverage by thioliates for C6T on Au(111)-(1 × 1) results in a value of 0.34 ML, in agreement with the value expected for one dense thiol monolayer on Au(111) substrate in the  $(\sqrt{3} \times \sqrt{3})R30^\circ$  phase ( $\theta_{thiolate} = 1/3$ ).<sup>63</sup> Taking into account the use of theoretical parameters, such as the differential photoemission cross sections,<sup>66</sup> and semi-empirical ones, such as the electron mean free path<sup>67</sup> or the gold lattice constant, we consider that the good agreement with accepted coverage values, entitled us to have a great confidence as regards to our calculations. We repeat the procedure for hexanethiol adsorbed on Au(001)-(1 × 1) surface, taking into account the different atomic density on this surface, obtaining a greater value for the coverage ( $\theta_{thiolate} \sim 0.4$  ML). This result is a bit larger than the one found for Au(111) substrate. This means that the ratio of the density of thiol molecules to the density of surface Au atoms in Au(001) is larger than in Au(111). The difference in coverage between the both Au faces arises from the larger number of Au surface atoms in the Au(111). A surface coverage  $\approx 0.4$  ML for Au(001)-(1×1) surface is slightly smaller than the one determined by electrochemical measurements in our recent publication (0.44),<sup>56</sup> which was assigned to  $\begin{pmatrix} 1 & -1 \\ 7 & 6 \end{pmatrix}$  and  $(2 \times 7)$  structures.<sup>68</sup> From the results achieved up to this point, we conclude that high quality hexanethiol SAMs are formed on both Au single-crystals surfaces, as it was already observed for closely packed and well-ordered alkanethiol SAMs on Au(111).<sup>64,69,70</sup>

### 3.2. Thermal desorption: Total S signal.

The study of desorption mechanisms of alkanethiol SAMs on gold surfaces in UHV conditions has an important drawback, i.e. thiulates on Au desorb in UHV (or vacuum) at room temperature. This means that the results can be seriously affected by the time elapsed between the sample introduction and the measurement starting. Thus, to investigate the chemical stability and the desorption process of these thiol SAMs we first survey the coverage evolution of C6T molecules as a function of the storage time in an UHV chamber ( $10^{-10}$  mbar) at RT. Additionally, we evaluate the effect of the type of substrate in this process using preferred oriented Au(111) polycrystalline and single-crystal Au(001)-(1 × 1). In a second step, we monitor the temporal evolution at different sample temperatures, in the range of 340 - 380 K, of the distinct species present in the hexanethiol SAMs on gold single-crystals, i.e.  $S_{A(\text{physisorbed})}$ ,  $S_{B(\text{thiolate})}$  and  $S_{C(\text{sulfide})}$ . In doing these experiments, we use XPS and perform the first ( $t_0$ ) measurement immediately after introducing the samples in the UHV chamber. The time required for transferring the SAMs/substrates from ethanolic solution to the UHV chamber is less than 20 minutes.

In Figure 2, we show the evolution of the total intensity ratio of S 2p and Au 4f, i.e. corresponding to the sum contributions of all forms of sulfur, for C6T SAMs on both gold surfaces at three different temperatures. While full symbols correspond to  $S_{\text{Total}}/\text{Au}$  intensity ratio for Au(111)-(1 × 1) substrate, empty ones are reserved to unreconstructed Au(001)-(1 × 1). Different shapes are for different temperatures; thus, circles are for RT, squares for  $T = 340$  K and triangles for  $T = 360$  K. While the time involved in the RT desorption is in the range of days and at higher temperatures in the range hours and minutes, the samples are under irradiation for minutes each experiment. In order to check the X-rays effect along the experiments, we take several consecutive measurements and compare the evolution of these spectra along time. Since we did not appreciate any change for long times of irradiation exposures (but short ones as compared to RT desorption times), we are sure that the X-rays bombardment, within our experimental conditions, does not alter the C6T SAMs. This result suggests that desorption is a natural independent process that is thermally induced.

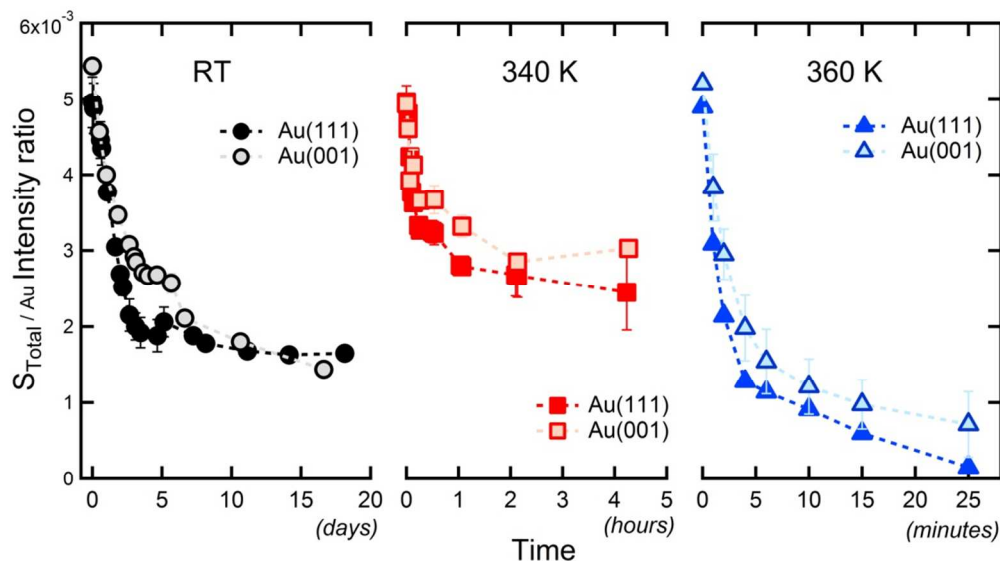


**Figure 2:**  $S_{\text{Total}}/\text{Au}$  intensity ratio as a function of annealing time at RT (days), 340 K (hours) and 360 K (min) in UHV conditions for hexanethiol SAMs on the Au(111)-(1 × 1) (full symbols) and Au(001)-(1 × 1) surfaces (open symbols).

The comparisons of these three time evolutions allowed us to make some immediate remarks: *i*) Open symbols are generally above full ones leading us to conclude that Au(001)-(1 × 1) face surface favours more stable alkanethiol SAMs growth. *ii*) The dynamical system reaches a stable, or at least metastable, stage at  $T = 340$  K characterized by a larger  $S$  coverage as compared to both at RT and at  $T = 360$  K.

*i*) In a recent work<sup>56</sup>, we found that the electrochemical desorption of C6T monolayers on Au(001) single crystal is shifted  $\approx 0.07$  V toward higher potentials, as compared to (111) one, showing that thiols SAMs are more stable over the less compact face, in agreement with molecular adsorption data on gold surfaces.<sup>71</sup> For the hexanethiol SAMs on the preferentially oriented (111) polycrystalline Au substrate at RT, a quick  $S$  species desorption is followed by a quite long steady state which contrasts with the slower but sustained C6T desorption on Au(001)-(1 × 1) surface. This particular evolution on Au(111) occurring at RT will be discussed deeper in the next section.

*ii*) It is known that a mild annealing process is required after the deposition for many organic self-assembled systems to fully order the arrangement.<sup>1,35</sup> This is due to the relative

1  
2  
3 ease, depending on the system, with which kinetically trapped configurations are achieved.  
4  
5 To overcome these kinds of configurations, and bring the system to a true minimum in the  
6  
7 Gibbs energy, some boost must be provided (in the form of  $KT$ ) to surmount the activation  
8  
9 barriers. This more ordered state of the SAMs can, in turn, optimize the van der Waals  
10  
11 landscape for each individual molecule and thus exhibit more reluctance to the desorption  
12  
13 and destabilization of the so self-assembled monolayers. However, the exposure of this  
14  
15 system to a slightly higher thermal energy, for instance  $T = 360$  K, can rapidly cause the  
16  
17 destruction of the C6T SAMs, as it is shown in Figure 2 and we will discuss in the  
18  
19 following section.  
20  
21

### 22 3.3. Chemistry of the SAMs desorption.

23  
24 To obtain information about the kinetics of the desorption and the chemical reaction  
25  
26 governing the process at different temperatures, we use the area of S 2p components ( $S_A$ ,  
27  
28  $S_B$  and  $S_C$ ) at every point in the isothermal desorption curves. This analysis allowed us to  
29  
30 explore the evolution of the different chemical species present in C6T SAMs along the  
31  
32 process for both substrates. As we previously stated, these species are the physisorbed one  
33  
34 ( $S_{A(\text{physisorbed})/\text{Au}}$ ) and both chemisorbed species ( $S_{B(\text{thiolate})/\text{Au}}$  and  $S_{C(\text{sulfide})/\text{Au}}$ ). By  
35  
36 surveying the intensities ratio (normalized to Au 4f intensity) of each one in the desorption  
37  
38 process, we are able to access to the mechanism behind the over-all process. In contrast  
39  
40 with the usual TPD experiments, providing information about the desorbing species, XPS  
41  
42 data give us the amount of S species remaining in the surface at a given time and  
43  
44 temperature, and are representative of the hexanethiolate surface coverage ( $\theta_{\text{thiolate}}$ ). As it is  
45  
46 conventional for the identification of Arrhenius type desorption kinetics (particularly when  
47  
48 it is suspected to be of first order), we show the total S 2p/Au 4f ratio in a logarithmic scale.  
49

- 50 • **Desorption at RT:**

51  
52 To begin this analysis, we chose the simplest case i.e. RT thermal desorption in  
53  
54 UHV conditions ( $10^{-10}$  mbar). In Figure 3, we depict the evolution of the different  
55  
56 components of S 2p spectrum occurring along several days ( $\sim 25 \times 10^3$  min). The results  
57  
58  
59  
60

corresponding to preferred oriented Au(111) polycrystalline and single-crystal Au(001)-(1 × 1) are depicted in the left (panel a) and the right (panel b) columns respectively. The species are associated, as previously discussed, to the physisorbed molecules ( $S_A$  circles) and the chemisorbed thiulates ( $S_B$  diamonds). The sum of  $S_A/Au$  and  $S_B/Au$  intensities ratios, for both substrates, is also shown in both figures ( $S_{Total}/Au$  square symbols). This last result was already shown in Figure 2, and it is repeated here to facilitate the discussion.

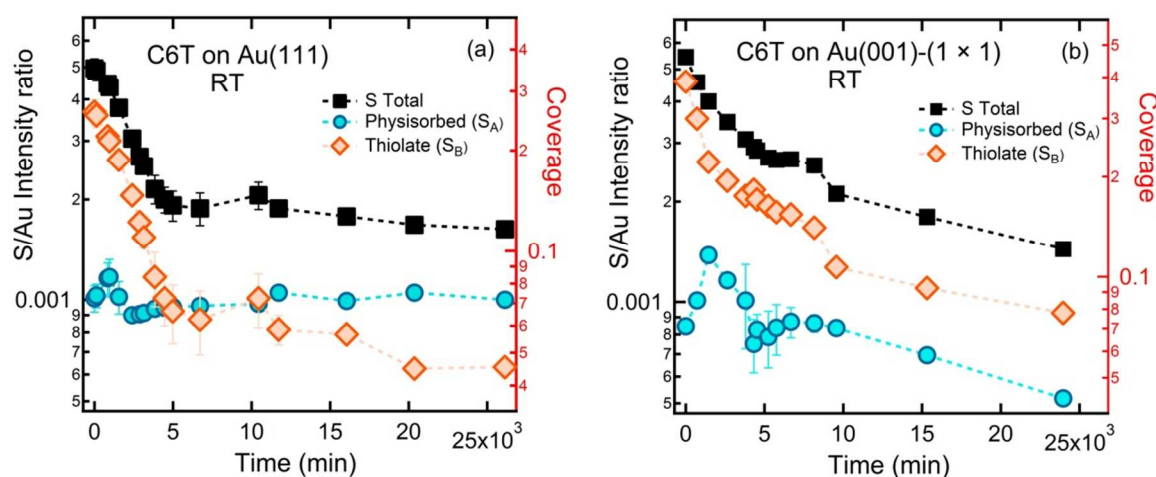


**Figure 3:**  $S_{Total}/Au$ ,  $S_{A(physisorbed)}/Au$  and  $S_{B(thiolate)}/Au$  intensity ratio as a function of storage time in UHV conditions at RT for hexanethiol SAMs on the preferred oriented Au(111)-(1 × 1) polycrystalline substrate (a) and Au(001)-(1 × 1) single-crystal surfaces (b).

At first glance, we observe that the total S 2p signal for C6T-Au(111) and C6T-Au(001) systems evolutions exhibits the same two stage decreasing trend. The fast initial decrease of the  $S_{Total}/Au$  ratio on both surfaces shows that the monolayer changes significantly with time at RT. At the end of the first stage (~4500 minutes), estimates of the total S amount vary in percentage depending on the Au face, 39% for Au(111) and 50% for Au(001)-(1 × 1). These results show that the spontaneous desorption is faster on the compact face. Above 5000 minutes, the C6T SAMs desorption kinetic becomes slower. Finally, after 17 days ( $2.5 \times 10^4$  min) storage in UHV at RT, the total S 2p signal detected was around 33% for both substrates.

1  
2  
3  
4  
5  
6  
7  
8  
9  
10  
11  
12  
13  
14  
15  
16  
17  
18  
19  
20  
21  
22  
23  
24  
25  
26  
27  
28  
29  
30  
31  
32  
33  
Although the first impression may suggest that desorption from both Au substrates is rather similar, a more careful analysis of the chemistry of each SAM shows some differences. The chemisorbed  $S_B$  species ( $C_6S-Au$ ) on the preferred oriented (111) polycrystalline Au desorbs according to a seemingly two stage kinetics; one with a faster rate that dominates the process in the initial 5000 minutes, and a slower one for longer desorption times. The first stage is faster for the (111) substrate compared with the (001) single-crystal. The amount of hexanethiolates ( $S_B$ ) is higher on Au(001) surface than the one on Au(111) at ~4500 minutes. The decrease of 75% ML of C6T molecules on (111) ( $\theta_{\text{thiolate}} \sim 0.07$  ML), against the 60% ML on the (001) face ( $\theta_{\text{thiolate}} \sim 0.15$  ML), supports the idea that the SAMs on unreconstructed Au(001)-(1 × 1) surface are more stable thermally than those on Au(111). Through DFT calculations and STM measurement,<sup>68</sup> Grumelli et al also probed that C6T SAMs on Au(001)-(1 × 1) are thermodynamically more stable than their Au(111)-(1 × 1) counterpart. On the other hand, a feature common to both systems is the initial onset of the intensity of  $S_A/Au$  ratio (S-S, S-H). After 1400 min, the desorption of the physisorbed  $S_A$  species is monotone only in the case of the Au(001) single-crystal. For the SAM on the preferred oriented (111) polycrystalline Au, after a brief quick descent, this species remains approximately constant up to the end.

34  
35  
36  
37  
38  
39  
40  
41  
42  
43  
44  
45  
46  
47  
48  
49  
50  
51  
52  
53  
54  
55  
56  
57  
58  
59  
60  
To explain the differences in the evolution of the chemistry of the SAMs in both substrates, we considered three assumptions: *i*) the interconversion between sulfur species, *ii*) the probability of desorption of each one, and *iii*) the dissimilarity in the crystallinity of the gold substrates i.e. preferred oriented (111) polycrystalline substrate vs. single-crystal.

*i*) A simple model may consider the direct desorption of the hexanethiolate species ( $C_6H_{13}S-Au$ ) directly to the gas face. However, it has been shown that a mechanism involving the formation (and later desorption) of disulfide species ( $C_6H_{13}S-S-C_6H_{13}$ ) from two thiulates is a more energetically favored alternative.<sup>39,55</sup>

*ii*) Initially, in the presence of the strongly surface attached thiolate species, not only the disulfides but also free thiol molecules (trapped during the formation of the SAM) may be retained through vdW interactions in between their respective alkyl chains.<sup>72</sup> This condition may explain the initial onset in the  $S_{A(\text{physisorbed})}$  intensity. But as the desorption proceeds, the thiulates ( $S_{B(\text{thiolate})}$ ) concentration falls and with that does the retaining effect of the



1  
2  
3 physisorbed species. At low coverage, disulfide molecules produced by recombination of  
4 thiolates may remain physisorbed<sup>72</sup> on the surface and prone to desorption.<sup>8</sup> For longer  
5 desorption times a less dense lying-down phase may result stabilized by both lateral inter-  
6 chain vdW and chain-gold substrate interactions.<sup>35</sup> The on-going desorption process  
7 competes with the diffusion and self-organization of the lying-down phase. At low  
8 temperatures (such as RT) the dominance of the desorption may result in the formation of a  
9 disordered and sparse lying-down phase. In any case, it is reasonable to think that the  
10 physisorbed molecules ( $S_A$ ) are quite more mobile than the thiolate ones ( $S_B$ ).  
11

12  
13  
14  
15  
16  
17  
18 *iii*) The preferred oriented (111) Au substrate is composed by small crystallites. The  
19 movement and pinning of the mobile physisorbed molecules at low coverages in the grain  
20 boundaries (that constitutes a major disruption to the crystalline lattice) is a possibility.  
21 This phenomenon may explain the additional amount of physisorbed species ( $S_A$ ) trapped  
22 on the surface in comparison with the Au(001) single-crystal. A compact hexagonal  $c(4 \times$   
23  $2)$  phase composed of long-chained disulfides on Au(111) have been reported<sup>73</sup> and later  
24 proven not to be the general case.<sup>63</sup> The existence of such informed arrangement is  
25 compatible with our observations and may be grounded on the use of a preferred oriented  
26 (111) polycrystalline Au as substrate.  
27  
28  
29  
30  
31  
32  
33  
34  
35  
36

37 • **Desorption at T = 340 K:**

38  
39 To avoid any non-uniformity in the surface defects, we performed the thermal  
40 induced desorption using single-crystals surfaces instead of preferred oriented (111)  
41 polycrystalline Au substrates. The C6T SAMs/substrates are heated at this fixed  
42 temperature during certain time, from 2 minutes to several hours, and then rapidly cooled  
43 down to RT to acquire the Au 4f<sub>7/2</sub>, S 2p and C 1s XPS spectra. In Figure 4, the time  
44 evolution of the all sulfur ( $S_{A(\text{physisorbed})}/\text{Au}$  and  $S_{B(\text{thiolate})}/\text{Au}$ ) species on Au(111) (a) and  
45 Au(001)-(1 × 1) (b) surfaces at a constant temperature of 340 K in UHV is shown. The  
46  $S_{\text{Total}}/\text{Au}$  ratio was already shown in Figure 2 (red square symbols).  
47  
48  
49  
50  
51  
52  
53  
54  
55  
56  
57  
58  
59  
60

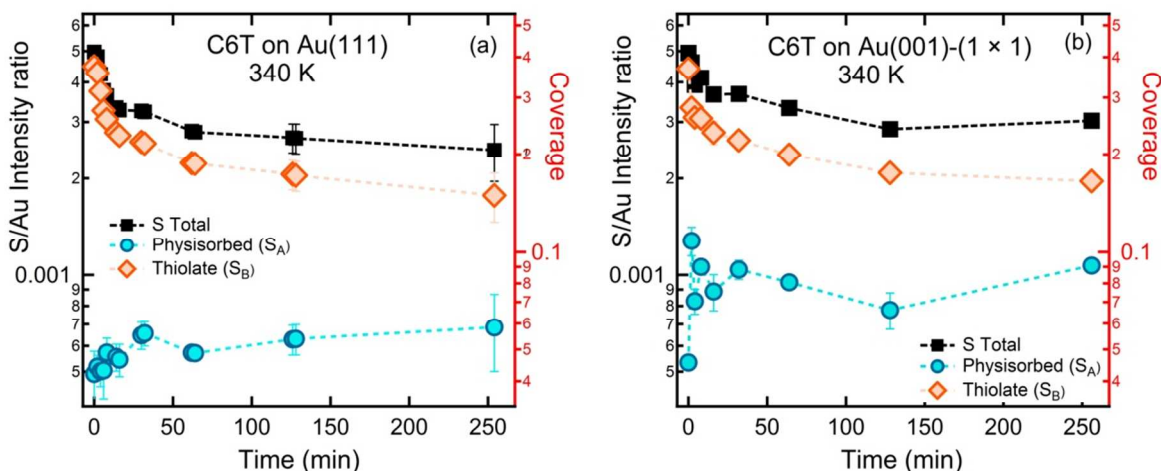


**Figure 4:**  $S_{\text{Total}}/\text{Au}$ ,  $S_{\text{A(Physisorbed)}}/\text{Au}$  and  $S_{\text{B(thiolate)}}/\text{Au}$  intensity ratio as a function of annealing time at 340 K in UHV conditions for C6T monolayers on the Au(111)-(1 × 1) (a) and Au(001)-(1 × 1) (b) single-crystals surfaces.

The hexanethiol SAMs desorption kinetic at  $T = 340$  K is independent of the Au single-crystal face. In both cases the total amount of S, dominated by the intensity of the hexanethiolate ( $S_B$ ) species, drops quickly reaching a stable, or at least metastable, state. The component of the physisorbed species ( $S_A$ ) increases quickly at the first stages, as in the RT experiments, but no drop of its intensity is observed in this case. As in the case of preferred oriented (111) polycrystalline Au substrates, the amount of all species reaches an approximately constant value but with the thiolate ( $S_B$ ) component still dominating. From these evolutions, we can speculate that the rise in the available thermal energy at an early stage, i.e. when the coverage is still high, may shake the system out of kinetic traps. This effect can, for instance, reorient the alkyl chains maximizing the vdW interactions between them, favoring the storage of the otherwise prone to diffusion/desorption physisorbed molecules (as disulfides). The effect of a mild annealing is known to drive SAMs closer to the thermodynamic steady state.<sup>35</sup> On the other hand, the short-chain (C6T and C8T) thiols on Au(111) are more defective (untilting and gauche defects) untilt rapidly at lower temperatures when compared to long-chains and, thus, are rendered structurally insensitive to further changes in temperature, in the temperature range of 300-390 K.<sup>74</sup> The ability of

1  
2  
3 short-chain SAMs to retain order with increasing thermal perturbations is governed by the  
4 inherently greater state of disorder prior to heat treatment.  
5  
6

7 This situation, in contrast with that at RT, clearly differs in origin for the  
8 physisorbed species. In the case of the RT study, we use preferred oriented (111)  
9 polycrystalline Au whose defects, i.e. abundant grain boundaries, act as residence sites for  
10 unbound species. At  $T = 340$  K, on the other hand, the retaining effects are provided by the  
11 vdW interactions in between alkylic chains, whether of thiolates or unbound molecules  
12 (e.g. disulfides) and with the substrate in an optimized arrangement. This is clear in  
13 comparing the evolution for C6T/Au(001)-(1 × 1), which is the same substrate (single-  
14 crystal) for both evolutions.  
15  
16  
17  
18  
19  
20  
21

22 The C6T SAMs coverage is larger on the (001) face than on (111) ones during the  
23 whole desorption experiment at  $T = 340$  K. After 4 hours of heating at this temperature, the  
24  $\theta_{\text{thiolate}}$  is around 40% ML for Au(111) ( $\theta_{\text{thiolate}} \approx 0.13$  ML) and 45% ML for Au(001)  
25 substrate ( $\theta_{\text{thiolate}} \approx 0.17$  ML). In this case, unlike the one at RT, the sudden desorption (at a  
26 higher coverage) may produce the formation of a more ordered and compact lying-down  
27 striped phase.<sup>35,75</sup> In fact, the coverage expected for C6T molecules in lying-down  
28 configuration on the Au(111) surface ( $\theta_{\text{thiolate}} = 1/8$  and  $2/15$ )<sup>76</sup> is very close to the surface  
29 coverage by thiolates reached in the nearly constant region. The plateau in the desorption  
30 curve at RT for Au(001) could correspond to the formation of a lying-down phase. At RT  
31 this effect is not observed in the (111) polycrystalline substrate because the desorption (or  
32 conversion to disulfide) takes place from a kinetically trapped situation with the thermal  
33 energy unable to surmount the transition to a compact lying-down arrangement for the  
34 SAM.  
35  
36  
37  
38  
39  
40  
41  
42  
43  
44  
45  
46  
47  
48  
49  
50  
51  
52  
53  
54  
55  
56  
57  
58  
59  
60

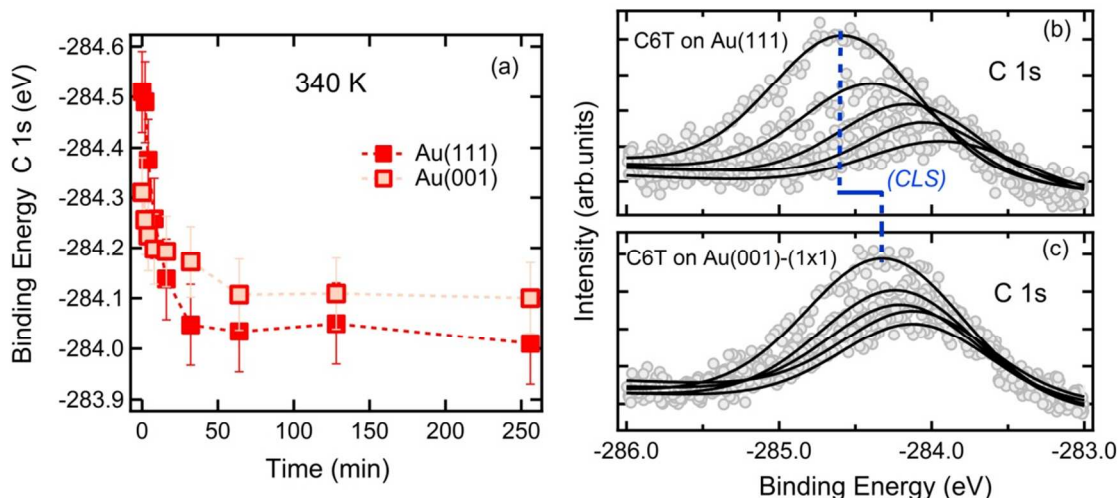


**Figure 5.** (a) BE of C 1s peak as a function of annealing time at 340 K in UHV conditions for hexanethiol SAMs on the Au(111)-(1 × 1) (full symbols) and Au(001)-(1 × 1) surfaces (open symbols). (b) Comparison of C 1s XPS spectra for C6T SAMs on Au(111) and (c) Au(001) obtained after a incubation of 24 h in a 100 μM ethanolic solution and in the course of the thermal desorption to 340 K. Also shown the best fit spectra as a solid black line.

To understand the behavior of the monolayers in the course of the thermal desorption, we also examine the evolution of the C 1s signal. A simple fitting to the detailed C 1s XPS spectra are performed using a linear background and two Voigt-like line shapes with the Lorentzian width fixed at 0.18 eV. The binding energy scale in C 1s spectra is referenced to the bulk Au  $4f_{7/2}$  peak at 84.00 eV. We subtract the component corresponding to the spurious C species from the full spectrum (with a constant BE  $\sim 285.1$  eV and a fwhm = 2.5 eV for both cases). In Figure 5 (a), we show the evolution of the photoemission signal BE for the molecular C in the SAMs on both gold surfaces at  $T = 340$  K. Figures 5 (b) and (c) show a series of C 1s XPS spectra for C6T chemisorbed on both unreconstructed surfaces: Au(111)-(1 × 1) (up) and Au(001)-(1 × 1) (down), obtained at different desorption times (0, 4, 16, 64 and 256 min). At saturated coverage, the C 1s signal on the Au(111) exhibit a single emission at  $(284.5 \text{ eV} \pm 0.08) \text{ eV}$ , in accordance with literature data.<sup>69,77</sup> The form of the peak for chemisorbed C6T molecules on the Au(001)-(1 × 1) surface is quite similar to that for the films prepared on Au(111), but the BE of this emission is  $\sim 0.2$  eV lower ( $(284.3 \text{ eV} \pm 0.07) \text{ eV}$ ), as in the case of the S 2p signals. This C

1  
2  
3  
4  
5  
6  
7  
8  
9  
10  
11  
12  
13  
14  
15  
16  
17  
18  
19  
20  
21  
22  
23  
24  
25  
26  
27  
28  
29  
30  
31  
32  
33  
34  
35  
36  
37  
38  
39  
40  
41  
42  
43  
44  
45  
46  
47  
48  
49  
50  
51  
52  
53  
54  
55  
56  
57  
58  
59  
60

1s emission is associated with the alkyl backbone of C6T SAMs on Au(111) in a standing-up configuration.<sup>69,77</sup> The evolution of the C 1s signals suggests that the configuration of the SAMs changes during the desorption. For both gold faces, the C 1s XPS peak shifts slightly toward lower values of binding energies and decreases in intensity as the annealing time is progressed. The corresponding Gaussian width remains approximately constant during the evolution for both cases ( $\sim 1$  eV), suggesting a single component in the whole process. The CLS is  $(0.5 \pm 0.08)$  eV for C6T on Au(111) and  $(0.2 \pm 0.07)$  eV for C6T on Au(001) reaching, within our experimental uncertainty, the same value. The downward shift BE is associated with the transformation from the standing-up configuration to a lying-down one,<sup>78</sup> and the gradual intensity decrease with the desorption of the thiol molecules. This result supports our model suggesting that the effect of the mild annealing is to lead to a metastable state in which the C6T molecules on Au surfaces are in a lying-down orientation. The lying-down phases have not been reported on the Au(001) surface, thus within this context, and taking into account that independent measurements, like STM ones, should be performed, our data could be the first evidence that they are also present on this substrate.

- **Desorption at higher temperatures (HT):**

When desorption temperatures are set at higher values ( $T = 360$  K and  $T = 380$  K), a much faster C6T SAMs desorption process takes place as indicated by triangle symbols in Figure 2 ( $T = 360$  K). The main feature of these HT desorption processes is the appearance of a new S species at a binding energy of S  $2p_{3/2} \sim 161.0$  eV denoted as  $S_{C(\text{sulfide})}$ ; this S  $2p_{3/2}$  BE has been assigned to monomeric sulfur chemisorbed to Au.<sup>61,62,64</sup> In Figure 6, we show the deconvolution in distinct species of the S 2p XPS signals in the initial stage of the C6T SAM on Au(001)-(1  $\times$  1) (on top) and after 6 minutes of annealing at  $T = 360$  K in UHV conditions (on the bottom). The heating process changes significantly the total S 2p peak area. The dominant  $S_B$  XPS component corresponding to chemisorbed hexanethiolates on Au and the  $S_{A(\text{physisorbed})}$  species, both present in well-ordered C6T SAMs on Au(001), become undetectable after 6 min at  $T = 360$  K. At this time, a different chemisorbed sulfur peak ( $S_{C(\text{sulfide})}$ ) is observed at a BE of  $(161.04 \pm 0.08)$  eV (S  $2p_{3/2}$ ). Although this doublet

has often appeared with alkanethiol SAMs of low molecular density or a disordered phase,<sup>37</sup> it is more likely that the cleavage of C-S bond of the thiol molecules is the responsible of the S-Au sulfide appearance, in agreement with previous reports.<sup>55,78</sup> As already reported in SAMs on Au(111), the atomically adsorbed sulfur can be desorbed completely at higher temperatures.<sup>78</sup>

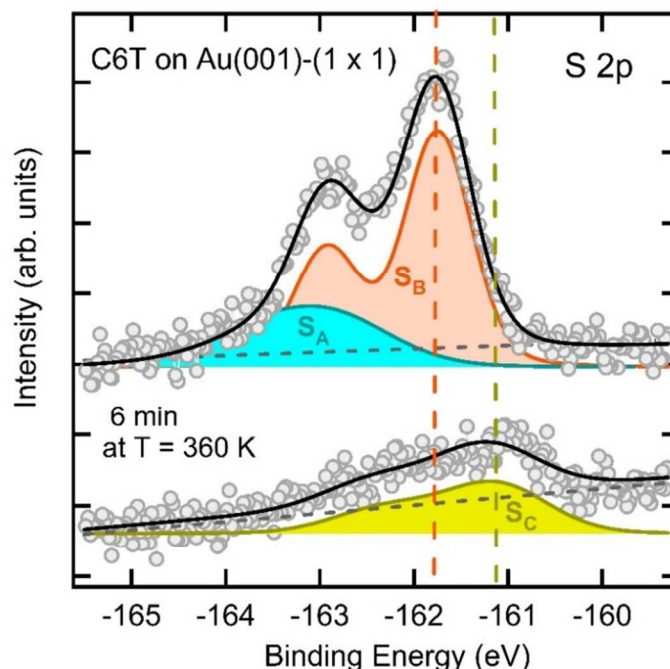


**Figure 6:** S 2p XPS spectra for the C6T SAM on Au(001)-(1×1) single-crystal obtained after a 24 h incubation and after annealing the sample 6 minutes at 360 K. Best fits (black line),  $S_A$ : physisorbed molecules (free R-SH, disulfide species (S-S bonds) or dialkylsulfide),  $S_B$ : chemisorbed thiolate,  $S_C$ : adsorbed sulfur when the C-S bond is broken.

In Figure 7 we depict the temporal evolution at  $T = 360$  K of the S 2p XPS signals (shown in Figure 6) normalized to Au 4f signals for the hexanethiol SAMs in both single-crystals (Au(111) (a) and Au(001)-(1 × 1) (b)). Both desorption curves follow a similar trend. We observe that the  $S_{A(\text{physisorbed})}$  and  $S_{B(\text{thiolate})}$  species significantly decreases until their complete disappearance at approximately 6 minutes for both faces. We need another

20 minutes of heating to completely desorb the  $S_{C(\text{sulfide})}$  remaining component (chemisorbed sulfur to Au). It should be noted that at high temperature (360 K) the variations in the quantities of the species of S are so fast that we missed the initial increasing of the  $S_{C(\text{sulfide})}$  signal which results of C6T SAM thermal decomposition.

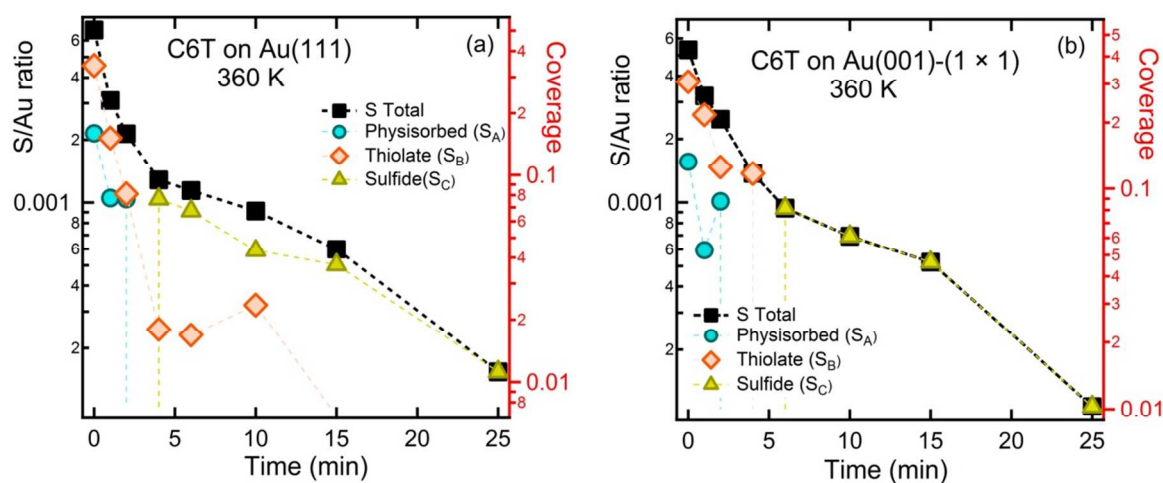


**Figure 7:**  $S_{\text{Total}}/\text{Au}$ ,  $S_{\text{A(physisorbed)}}/\text{Au}$ ,  $S_{\text{B(thiolate)}}/\text{Au}$  and  $S_{\text{C(sulfide)}}/\text{Au}$  intensity ratio as a function of annealing time at 360 K in UHV conditions for C6T monolayers on the Au(111)-(1 × 1) (a) and Au(001)-(1 × 1) surfaces (b).

It is important to remark that the cleavage of C-S bond takes place approximately at the same time (5-6 minutes), independently either of the evolution of each species or the substrate gold face. To confirm this trend, we perform an experiment at  $T = 380$  K. Figure 8 shows the deconvolution in species of the S 2p XPS signals in the initial stage of the C6T monolayer on Au(001)-(1 × 1) and after one minute of heating at 380 K in UHV chamber. We found that the S 2p XPS spectrum changed drastically. The annealing at this temperature of the hexanethiol SAMs on both Au surfaces result in a clear enhancement of the  $S_{C(\text{sulfide})}$  component, confirming our suggestion about the C-S bond cleavage. The bond C-S scission takes place even faster (60 seconds). This result agrees with what was found in the course of the thermal desorption of the stripe phase on Au(111),<sup>78</sup> i.e. the thiolate species evolves into atomic sulfur via C-S bond breaking, without detecting other sulfur species.



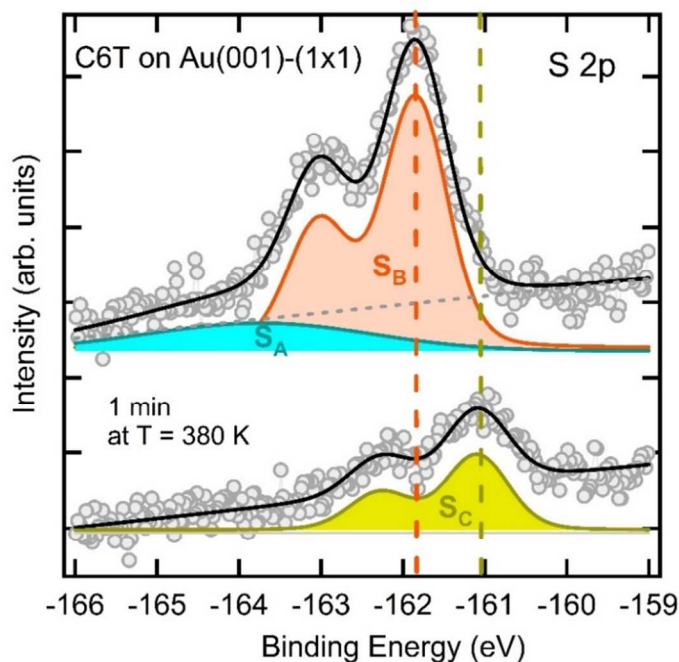


**Figure 8:** S 2p XPS spectra for the C6T SAM on Au(001)-(1 × 1) obtained after a 24 h incubation and after annealing the sample 1 minutes at T = 380 K. Best fits (black line), S<sub>A</sub>: physisorbed molecules (free R-SH, disulfide species (S-S bonds) or dialkylsulfide), S<sub>B</sub>: chemisorbed thiolate, S<sub>C</sub>: adsorbed sulfur when the C-S bond is broken.

## Conclusions

We carried out an XPS study of the thermal desorption of SAMs of C6T on unreconstructed Au(111) and Au(001) surfaces. We found that the initial surface coverage of the SAMs produced by adsorption from ethanolic solutions of *n*-hexanethiol on Au(001)-(1 × 1) is higher (~ 0.4 ML) than its counterpart formed on Au(111) substrate (~ 0.33 ML). Additionally, we found that the SAMs on the (001) face of Au are more stable to an isothermal treatment (in the range RT to T = 380 K) than the case of the (111) face. This is rooted in the experimental fact that, for any given probed temperature, the total amount of S is at the same time always greater for the SAMs on the Au(001)-(1 × 1) surface. These results are consistent with the two novel surface models recently proposed for C6T SAMs on the Au(001)-(1 × 1) surface.<sup>68</sup> The desorption process at room temperature is very slow



1  
2  
3 and is dominated by kinetic effects and the desorption of the hexanethiolate species through  
4 the formation of S-S or S-H containing species. This leads to a continuous desorption in the  
5 case of the Au(001) single-crystal substrates, whereas for the preferred oriented (111)  
6 polycrystalline Au the desorption produces remaining disulfide species probably pinned at  
7 the grain boundaries. On the other hand, at  $T = 340$  K both systems reach a metastable state  
8 with a coverage around  $\theta_{\text{thiolate}} \approx 0.13\text{-}0.17$  ML, which can be assigned to molecules in a  
9 lying-down configuration that have been reported in the Au(111) but, as far as we know,  
10 have not been observed on the Au(001) face. The difference may reside in the effect of a  
11 moderate annealing that drives the system into a thermodynamically controlled steady state.  
12 Even higher temperatures rapidly break the C-S bond in the C6T molecule producing  
13 chemisorbed S on both Au surfaces.  
14  
15  
16  
17  
18  
19  
20  
21  
22  
23  
24

## 25 **Acknowledgment**

26 The authors acknowledge financial support from ANPCyT (PICT 2321) from Argentina.  
27  
28  
29  
30  
31

## 32 **References**

- 33  
34  
35 (1) Love, J. C.; Estroff, L. A.; Kriebel, J. K.; Nuzzo, R. G.; Whitesides, G. M. Self-  
36 Assembled Monolayers of Thiolates on Metals as a Form of Nanotechnology.  
37 *Chem. Rev.* **2005**, *105*, 1103–1169.  
38  
39  
40 (2) Schreiber, F. Structure and Growth of Self-Assembling Monolayers. *Prog. Surf. Sci.*  
41 **2000**, *65*, 151–257.  
42  
43  
44 (3) Li, X.-M.; Huskens, J.; Reinhoudt, D. N. Reactive Self-Assembled Monolayers on  
45 Flat and Nanoparticle Surfaces, and Their Application in Soft and Scanning Probe  
46 Lithographic Nanofabrication Technologies. *J. Mater. Chem.* **2004**, *14*, 2954–2971.  
47  
48  
49 (4) Ulman, A. Formation and Structure of Self-Assembled Monolayers. *Chem. Rev.*  
50 **1996**, *96*, 1533–1554.  
51  
52  
53 (5) Poirier, G. E. Characterization of Organosulfur Molecular Monolayers on Au(111)  
54 Using Scanning Tunneling Microscopy. *Chem. Rev.* **1997**, *97*, 1117–1128.  
55  
56  
57  
58  
59  
60

- 1  
2  
3 (6) Krämer, S.; Fuierer, R. R.; Gorman, C. B. Scanning Probe Lithography Using Self-  
4 Assembled Monolayers. *Chem. Rev.* **2003**, *103*, 4367–4418.  
5  
6  
7 (7) Kind, M.; Wöll, C. Organic Surfaces Exposed by Self-Assembled Organothiols  
8 Monolayers: Preparation, Characterization, and Application. *Prog. Surf. Sci.* **2009**,  
9 *84*, 230–278.  
10  
11  
12 (8) Vericat, C.; Benitez, G. A.; Grumelli, D. E.; Vela, M. E.; Salvarezza, R. C. Thiol-  
13 Capped Gold: From Planar to Irregular Surfaces. *J. Phys. Condens. Matter* **2008**, *20*,  
14 184004–184012.  
15  
16  
17 (9) Bucher, J.-P.; Santesson, L.; Kern, K. Thermal Healing of Self-Assembled Organic  
18 Monolayers: Hexane- and Octadecanethiol on Au(111) and Ag(111). *Langmuir*  
19 **1994**, *10*, 979–983.  
20  
21  
22 (10) Kodama, C.; Hayashi, T.; Nozoye, H. Decomposition of Alkanethiols Adsorbed on  
23 Au (1 1 1) at Low Temperature. *Appl. Surf. Sci.* **2001**, *169–170*, 264–267.  
24  
25  
26 (11) Lavrich, D. J. .; Wetterer, S. M. .; Bernasek, S. L. .; Scoles, G. Physisorption and  
27 Chemisorption of Alkanethiols and Alkyl Sulfides on Au(111). *J. Phys. Chem. B*  
28 **1998**, *102*, 3456–3465.  
29  
30  
31 (12) Nishida, N.; Hara, M.; Sasabe, H.; Knoll, W. Formation and Exchange Processes of  
32 Alkanethiol Self-Assembled Monolayer on Au(111) Studied by Thermal Desorption  
33 Spectroscopy and Scanning Tunneling Microscopy. *Jpn. J. Appl. Phys.* **1997**, *36*,  
34 2379–2385.  
35  
36  
37 (13) Nuzzo, R. G.; Zegarski, B. R.; Dubois, L. H. Fundamental Studies of the  
38 Chemisorption of Organosulfur Compounds on gold(111). Implications for  
39 Molecular Self-Assembly on Gold Surfaces. *J. Am. Chem. Soc.* **1987**, *109*, 733–740.  
40  
41  
42 (14) Poirier, G. E. Butanethiol Self-Assembly on Au(001): The 1×4 Au Missing Row,  
43 c(2×8) Molecular Lattice. *J. Vac. Sci. Technol. B Microelectron. Nanom. Struct.*  
44 **1996**, *14*, 1453–1460.  
45  
46  
47 (15) Kondoh, H.; Kodama, C.; Sumida, H.; Nozoye, H. Molecular Processes of  
48 Adsorption and Desorption of Alkanethiol Monolayers on Au(111). *J. Chem. Phys.*  
49 **1999**, *111*, 1175.  
50  
51  
52  
53  
54  
55  
56  
57  
58  
59  
60

- 1  
2  
3  
4  
5  
6  
7  
8  
9  
10  
11  
12  
13  
14  
15  
16  
17  
18  
19  
20  
21  
22  
23  
24  
25  
26  
27  
28  
29  
30  
31  
32  
33  
34  
35  
36  
37  
38  
39  
40  
41  
42  
43  
44  
45  
46  
47  
48  
49  
50  
51  
52  
53  
54  
55  
56  
57  
58  
59  
60
- (16) Kondoh, H.; Kodama, C.; Nozoye, H. Structure-Dependent Change of Desorption Species from N-Alkanethiol Monolayers Adsorbed on Au(111): Desorption of Thiolate Radicals from Low-Density Structures. *J. Phys. Chem. B* **1998**, *102*, 2310–2312.
- (17) Daniel, M. C.; Astruc, D. Gold Nanoparticles: Assembly, Supramolecular Chemistry, Quantum-Size-Related Properties, and Applications toward Biology, Catalysis, and Nanotechnology. *Chem. Rev.* **2004**, *104*, 293–346.
- (18) Gittins, D. I.; Bethell, D.; Schiffrin, D. J.; Nichols, R. A Nanometre-Scale Electronic Switch Consisting of a Metal Cluster and Redox-Addressable Groups. *Nature* **2000**, *408*, 67–69.
- (19) Rosi, N. L.; Giljohann, D. A.; Thaxton, C. S.; Lytton-Jean, A. K. R.; Han, M. S.; Mirkin, C. A. Oligonucleotide-Modified Gold Nanoparticles for Intracellular Gene Regulation. *Science (80-. )*. **2006**, *312*, 1027–1030.
- (20) Beissenhirtz, M. K.; Elnathan, R.; Weizmann, Y.; Willner, I. The Aggregation of Au Nanoparticles by an Autonomous DNA Machine Detects Viruses. *Small* **2007**, *3*, 375–379.
- (21) Barnard, A. S.; Lin, X. M.; Curtiss, L. A. Equilibrium Morphology of Face-Centered Cubic Gold Nanoparticles >3 Nm and the Shape Changes Induced by Temperature. *J. Phys. Chem. B* **2005**, *109*, 24465–24472.
- (22) Barnard, A. S. Direct Comparison of Kinetic and Thermodynamic Influences on Gold Nanomorphology. *Acc. Chem. Res.* **2012**, *45*, 1688–1697.
- (23) Barnard, A. S.; Chen, Y. Kinetic Modelling of the Shape-Dependent Evolution of Faceted Gold Nanoparticles. *J. Mater. Chem.* **2011**, *21*, 12239–12245.
- (24) Barnard, A. S. Modeling the Impact of Alkanethiol SAMs on the Morphology of Gold Nanocrystals. *Cryst. Growth Des.* **2013**, *13*, 5433–5441.
- (25) Azcárate, J. C.; Corthey, G.; Pensa, E.; Vericat, C.; Fonticelli, M. H.; Salvarezza, R. C.; Carro, P. Understanding the Surface Chemistry of Thiolate-Protected Metallic Nanoparticles. *J. Phys. Chem. Lett.* **2013**, *4*, 3127–3138.

- 1  
2  
3 (26) Schreiber, F. Self-Assembled Monolayers: From Simple Model Systems to  
4 Biofunctionalized Interfaces. *J. Phys. Condens. Matter* **2004**, *16*, R881–R900.  
5  
6  
7 (27) Nuzzo, R. G.; Dubois, L. H.; Allara, D. L. Fundamental Studies of Microscopic  
8 Wetting on Organic Surfaces. 1. Formation and Structural Characterization of a Self-  
9 Consistent Series of Polyfunctional Organic Monolayers. *J. Am. Chem. Soc.* **1990**,  
10 *112*, 558–569.  
11  
12  
13  
14 (28) Turchanin, A.; Käfer, D.; El-Desawy, M.; Wöll, C.; Witte, G.; Götzhäuser, A.  
15 Molecular Mechanisms of Electron-Induced Cross-Linking in Aromatic SAMs.  
16 *Langmuir* **2009**, *25*, 7342–7352.  
17  
18  
19  
20 (29) Ito, E.; Noh, J.; Hara, M. Steric Effects on Adsorption and Desorption Behaviors of  
21 Alkanethiol Self-Assembled Monolayers on Au(111). *Chem. Phys. Lett.* **2008**, *462*,  
22 209–212.  
23  
24  
25  
26 (30) Käfer, D.; Witte, G.; Cyganik, P.; Terfort, A.; Wöll, C. A Comprehensive Study of  
27 Self-Assembled Monolayers of Anthracenethiol on Gold: Solvent Effects, Structure,  
28 and Stability. *J. Am. Chem. Soc.* **2006**, *128*, 1723–1732.  
29  
30  
31  
32 (31) Stettner, J.; Frank, P.; Griesser, T.; Trimmel, G.; Schennach, R.; Gilli, E.; Winkler,  
33 A. A Study on the Formation and Thermal Stability of 11-MUA SAMs on  
34 Au(111)/Mica and on Polycrystalline Gold Foils. *Langmuir* **2009**, *25*, 1427–1433.  
35  
36  
37  
38 (32) Yang, G.; Liu, G. New Insights for Self-Assembled Monolayers of Organothiols on  
39 Au(111) Revealed by Scanning Tunneling Microscopy. *J. Phys. Chem. B* **2003**, *107*,  
40 8746–8759.  
41  
42  
43  
44 (33) Lee, N.-S.; Kim, D.; Kang, H.; Park, D. K.; Han, S. W.; Noh, J. Structural  
45 Transitions of Octanethiol Self-Assembled Monolayers on Gold Nanoplates after  
46 Mild Thermal Annealing. *J. Phys. Chem. C* **2011**, *115*, 5868–5874.  
47  
48  
49  
50 (34) Camillone, N.; Eisenberger, P.; Leung, T. Y. B.; Schwartz, P.; Scoles, G.; Poirier, G.  
51 E.; Tarlov, M. J. New Monolayer Phases of N-Alkane Thiols Self-Assembled on  
52 Au(111): Preparation, Surface Characterization, and Imaging. *J. Chem. Phys.* **1994**,  
53 *101*, 11031–11036.  
54  
55  
56  
57 (35) Qian, Y.; Yang, G.; Yu, J.; Jung, T. A.; Liu, G. Structures of Annealed Decanethiol  
58  
59  
60

- 1  
2  
3 Self-Assembled Monolayers on Au(111): An Ultrahigh Vacuum Scanning Tunneling  
4 Microscopy Study. *Langmuir* **2003**, *19*, 6056–6065.
- 5  
6  
7 (36) Stettner, J.; Winkler, A. Characterization of Alkanethiol Self-Assembled Monolayers  
8 on Gold by Thermal Desorption Spectroscopy. *Langmuir* **2010**, *26*, 9659–9665.
- 9  
10  
11 (37) Ito, E.; Kang, H.; Lee, D.; Park, J. B.; Hara, M.; Noh, J. Spontaneous Desorption and  
12 Phase Transitions of Self-Assembled Alkanethiol and Alicyclic Thiol Monolayers  
13 Chemisorbed on Au(111) in Ultrahigh Vacuum at Room Temperature. *J. Colloid*  
14 *Interface Sci.* **2013**, *394*, 522–529.
- 15  
16  
17 (38) Maksymovych, P.; Voznyy, O.; Dougherty, D. B.; Sorescu, D. C.; Yates Jr., J. T.  
18 Gold Adatom as a Key Structural Component in Self-Assembled Monolayers of  
19 Organosulfur Molecules on Au(1 1 1). *Prog. Surf. Sci.* **2010**, *85*, 206–240.
- 20  
21  
22 (39) Hayashi, T.; Wakamatsu, K.; Ito, E.; Hara, M. Effect of Steric Hindrance on  
23 Desorption Processes of Alkanethiols on Au(111). *J. Phys. Chem. C* **2009**, *113*,  
24 18795–18799.
- 25  
26  
27 (40) Nishida, N.; Hara, M.; Sasabe, H.; Knoll, W. Thermal Desorption Spectroscopy of  
28 Alkanethiol Self-Assembled Monolayer on Au(111). *Jpn. J. Appl. Phys.* **1996**, *35*,  
29 5866–5872.
- 30  
31  
32 (41) Rzeźnicka, I. I.; Lee, J.; Maksymovych, P.; Yates, J. T. J. Nondissociative  
33 Chemisorption of Short Chain Alkanethiols on Au(111). *J. Phys. Chem. B* **2005**,  
34 *109*, 15992–15996.
- 35  
36  
37 (42) Poirier, G. E.; And, W. P. F.; White, J. M. Two-Dimensional Phase Diagram of  
38 Decanethiol on Au(111). *Langmuir* **2001**, *17*, 1176–1183.
- 39  
40  
41 (43) Ishida, T.; Fukushima, H.; Mizutani, W.; Miyashita, S.; Ogiso, K.; Ozaki, H.;  
42 Tokumoto, H. Annealing Effect of Self-Assembled Monolayers Generated from  
43 Terphenyl Derivatized Thiols on Au(111). *Langmuir* **2002**, *18*, 83–92.
- 44  
45  
46 (44) Yamada, R.; Wano, H. A.; Uosaki, K. Effect of Temperature on Structure of the  
47 Self-Assembled Monolayer of Decanethiol on Au(111) Surface. *Langmuir* **2000**, *16*,  
48 5523–5525.
- 49  
50  
51  
52  
53  
54  
55  
56  
57  
58  
59  
60

- 1  
2  
3 (45) Bondzie, V.; Dixon-warren, S. J.; Yu, Y.; Zhang, L. Adsorption and Desorption of  
4 Butanethiol on Au{100}-(5 × 20). *Surf. Sci.* **1999**, *431*, 174–185.  
5  
6  
7 (46) Castner, D. G.; And, K. H.; Grainger, D. W. X-Ray Photoelectron Spectroscopy  
8 Sulfur 2p Study of Organic Thiol and Disulfide Binding Interactions with Gold  
9 Surfaces. *Langmuir* **1996**, *12*, 5083–5086.  
10  
11  
12 (47) Moulder, J. F.; Stickle, W. F.; Sobol, P. E.; Bomben, K. D. Handbook of X-Ray  
13 Photoelectron Spectroscopy. *Chastain, J., Ed.; Perkin-Elmer Corp. Eden Prairie,*  
14 *MN* **1992**.  
15  
16  
17 (48) Cometto, F. P.; Ruano, G.; Ascolani, H.; Zampieri, G. Adlayers of Alkanedithiols on  
18 Au(111): Effect of Disulfide Reducing Agent. *Langmuir* **2013**, *29*, 1400–1406.  
19  
20  
21 (49) Cometto, F. P.; Ruano, G.; Soria, F. A.; Calderón, C. A.; Paredes-Olivera, P. A.;  
22 Zampieri, G.; Patrio, E. M. Thermal and Chemical Stability of N -Hexadecanethiol  
23 Monolayers on Au(111) in O<sub>2</sub> Environments. *Electrochim. Acta* **2016**, *215*, 313–  
24 325.  
25  
26  
27 (50) Cortés, E.; Rubert, A. a.; Benitez, G.; Carro, P.; Vela, M. E.; Salvarezza, R. C.  
28 Enhanced Stability of Thiolate Self-Assembled Monolayers (SAMs) on  
29 Nanostructured Gold Substrates. *Langmuir* **2009**, *25*, 5661–5666.  
30  
31  
32 (51) Duwez, A.-S. Exploiting Electron Spectroscopies to Probe the Structure and  
33 Organization of Self-Assembled Monolayers: A Review. *J. Electron Spectros. Relat.*  
34 *Phenomena* **2004**, *134*, 97–138.  
35  
36  
37 (52) Vericat, C.; Vela, M. E.; Salvarezza, R. C. Self-Assembled Monolayers of  
38 Alkanethiols on Au(111): Surface Structures, Defects and Dynamics. *Phys. Chem.*  
39 *Chem. Phys.* **2005**, *7*, 3258–3268.  
40  
41  
42 (53) Heister, H.; Zharnikov M.; Grunze, M.; Johansson, L. S. O. Adsorption of  
43 Alkanethiols and Biphenylthiols on Au and Ag Substrates: A High-Resolution X-  
44 Ray Photoelectron Spectroscopy Study. *J. Phys. Chem. B* **2001**, *105*, 4058–4061.  
45  
46  
47 (54) Himmel, H.-J.; Wöll, C.; Gerlach, R.; Polanski, G.; Rubahn, H.-G. Structure of  
48 Heptanethiolate Monolayers on Au(111): Adsorption from Solution vs Vapor  
49 Deposition. *Langmuir* **1997**, *13*, 602–605.  
50  
51  
52  
53  
54  
55  
56  
57  
58  
59  
60

- 1  
2  
3  
4  
5  
6  
7  
8  
9  
10  
11  
12  
13  
14  
15  
16  
17  
18  
19  
20  
21  
22  
23  
24  
25  
26  
27  
28  
29  
30  
31  
32  
33  
34  
35  
36  
37  
38  
39  
40  
41  
42  
43  
44  
45  
46  
47  
48  
49  
50  
51  
52  
53  
54  
55  
56  
57  
58  
59  
60
- (55) Liu, G.; Rodriguez, J. A.; Dvorak, J.; Hrbek, J.; Jirsak, T. Chemistry of Sulfur-Containing Molecules on Au(111): Thiophene, Sulfur Dioxide, and Methanethiol Adsorption. *Surf. Sci.* **2002**, *505*, 295–307.
- (56) Grumelli, D.; Cristina, L. J.; Maza, F. L.; Carro, P.; Ferrón, J.; Kern, K.; Salvarezza, R. C. Thiol Adsorption on the Au(100)-Hex and Au(100)-(1 × 1) Surfaces. *J. Phys. Chem. C* **2015**, *119*, 14248–14254.
- (57) Nilsson, D.; Watcharinyanon, S.; Eng, M.; Li, L.; Moons, E.; Johansson, L. S. O.; Zharnikov, M.; Shaporenko, A.; Albinsson, B.; Mårtensson, J. Characterization of Self-Assembled Monolayers of Oligo(phenyleneethynylene) Derivatives of Varying Shapes on Gold: Effect of Laterally Extended  $\pi$ -Systems. *Langmuir* **2007**, *23*, 6170–6181.
- (58) Watcharinyanon, S.; Nilsson, D.; Moons, E.; Shaporenko, A.; Zharnikov, M.; Albinsson, B.; Mårtensson, J.; Johansson, L. S. O.; Carravetta, V.; Mårtensson, J.; et al. A Spectroscopic Study of Self-Assembled Monolayer of Porphyrin-Functionalized Oligo(phenyleneethynylene)s on Gold: The Influence of the Anchor Moiety. *Phys. Chem. Chem. Phys.* **2008**, *10*, 5264.
- (59) Heister, K.; Zharnikov, M.; Grunze, M.; Johansson, L. S. O.; Ulman, A. Characterization of X-Ray Induced Damage in Alkanethiolate Monolayers by High-Resolution Photoelectron Spectroscopy. *Langmuir* **2000**, *17*, 8–11.
- (60) Zharnikov, M. High-Resolution X-Ray Photoelectron Spectroscopy in Studies of Self-Assembled Organic Monolayers. *J. Electron Spectros. Relat. Phenomena* **2010**, *178–179*, 380–393.
- (61) Rodriguez, J. a.; Dvorak, J.; Jirsak, T.; Liu, G.; Hrbek, J.; Aray, Y.; González, C. Coverage Effects and the Nature of the Metal-Sulfur Bond in S/Au(111): High-Resolution Photoemission and Density-Functional Studies. *J. Am. Chem. Soc.* **2003**, *125*, 276–285.
- (62) Jiang, Y.; Liang, X.; Ren, S.; Chen, C.-L.; Fan, L.-J.; Yang, Y.-W.; Tang, J.-M.; Luh, D.-A. The Growth of Sulfur Adlayers on Au(100). *J. Chem. Phys.* **2015**, *142*, 064708/1-11.

- 1  
2  
3 (63) Vericat, C.; Vela, M. E.; Benitez, G.; Carro, P.; Salvarezza, R. C. Self-Assembled  
4 Monolayers of Thiols and Dithiols on Gold: New Challenges for a Well-Known  
5 System. *Chem. Soc. Rev.* **2010**, *39*, 1805–1834.  
6  
7  
8  
9 (64) Ishida, T.; Choi, N.; Mizutani, W.; Tokumoto, H.; Kojima, I.; Azebara, H.; Hokari,  
10 H.; Akiba, U.; Fujihira, M. High-Resolution X-Ray Photoelectron Spectra of  
11 Organosulfur Monolayers on Au(111): S(2p) Spectral Dependence on Molecular  
12 Species. *Langmuir* **1999**, *15*, 6799–6806.  
13  
14  
15  
16 (65) Ishida, T.; Hara, M.; Kojima, I.; Tsuneda, S.; Nishida, N.; Sasabe, H.; Knoll, W.  
17 High Resolution X-Ray Photoelectron Spectroscopy Measurements of  
18 Octadecanethiol Self-Assembled Monolayers on Au(111). *Langmuir* **1998**, *14*,  
19 2092–2096.  
20  
21  
22  
23 (66) Yeh, J. J.; Lindau, I. Atomic Subshell Photoionization Cross Sections and  
24 Asymmetry Parameters:  $1 < Z < 103$ . *At. Data Nucl. Data Tables* **1985**, *32*, 1–155.  
25  
26  
27 (67) Afeefy, H. Y.; Liebman, J. F.; Stein, S. E. NIST Electron Inelastic-Mean-Free-Path  
28 Database: Version 1.2. NIST Standard Reference Database 71 | NIST  
29 <https://www.nist.gov/srd/nist-standard-reference-database-71> (accessed Sep 5, 2017).  
30  
31  
32  
33 (68) Grumelli, D.; Maza, F. L.; Kern, K.; Salvarezza, R. C.; Carro, P. Surface Structure  
34 and Chemistry of Alkanethiols on Au(100)-(1 × 1) Substrates. *J. Phys. Chem. C*  
35 **2016**, *120*, 291–296.  
36  
37  
38  
39 (69) Chesneau, F.; Zhao, J.; Shen, C.; Buck, M.; Zharnikov, M. Adsorption of Long-  
40 Chain Alkanethiols on Au(111): A Look from the Substrate by High Resolution X-  
41 Ray Photoelectron Spectroscopy. *J. Phys. Chem. C* **2010**, *114*, 7112–7119.  
42  
43  
44  
45 (70) Ito, E.; Noh, J.; Hara, M. Steric Effects on Adsorption and Desorption Behaviors of  
46 Alkanethiol Self-Assembled Monolayers on Au(111). *Chem. Phys. Lett.* **2008**, *462*,  
47 209–212.  
48  
49  
50  
51 (71) Carabineiro, S. A. C.; Nieuwenhuys, B. E. Adsorption of Small Molecules on Gold  
52 Single Crystal Surfaces. *Gold Bull.* **2009**, *42*, 288–301.  
53  
54  
55  
56 (72) Cometto, F. P.; Calderón, C. A.; Berdakin, M.; Paredes-Olivera, P.; Macagno, V. A.;  
57 Patrito, E. M. Electrochemical Detection of the Thermal Stability of N-  
58  
59  
60



- 1  
2  
3 Alkanethiolate Monolayers on Au(111). *Electrochim. Acta* **2012**, *61*, 132–139.  
4  
5  
6 (73) Fenter, P.; Eberhardt, A.; Eisenberger, P. Self-Assembly of N-Alkyl Thiols as  
7 Disulfides on Au(111). *Science*, **1994**, *266*, 1216–1218.  
8  
9  
10 (74) Prathima, N.; Harini, M.; Neeraj Rai; Chandrashekara, R. H.; Ayappa, K. G.;  
11 Sampath, S.; Biswas, S. K. Thermal Study of Accumulation of Conformational  
12 Disorders in the Self-Assembled Monolayers of C8 and C18 Alkanethiols on the  
13 Au(111) Surface. *Langmuir* **2005**, *21*, 2364–2374.  
14  
15  
16  
17 (75) Guo, Q.; Li, F. Self-Assembled Alkanethiol Monolayers on Gold Surfaces:  
18 Resolving the Complex Structure at the Interface by STM. *Phys. Chem. Chem. Phys.*  
19 **2014**, *16*, 19074.  
20  
21  
22  
23 (76) Löfgren, J.; Grönbeck, H.; Moth-Poulsen, K.; Erhart, P. Understanding the Phase  
24 Diagram of Self-Assembled Monolayers of Alkanethiolates on Gold. *J. Phys. Chem.*  
25 *C* **2016**, *120*, 12059–12067.  
26  
27  
28  
29 (77) Hamoudi, H.; Chesneau, F.; Patze, C.; Zharnikov, M. Chain-Length-Dependent  
30 Branching of Irradiation-Induced Processes in Alkanethiolate Self-Assembled  
31 Monolayers. *J. Phys. Chem. C* **2011**, *115*, 534–541.  
32  
33  
34  
35 (78) Yang, Y. W.; Fan, L. J. High-Resolution XPS Study of Decanethiol on Au(111):  
36 Single Sulfur–Gold Bonding Interaction. *Langmuir* **2002**, *18*, 1157–1164.  
37  
38  
39  
40  
41  
42  
43  
44  
45  
46  
47  
48  
49  
50  
51  
52  
53  
54  
55  
56  
57  
58  
59  
60

## Figures

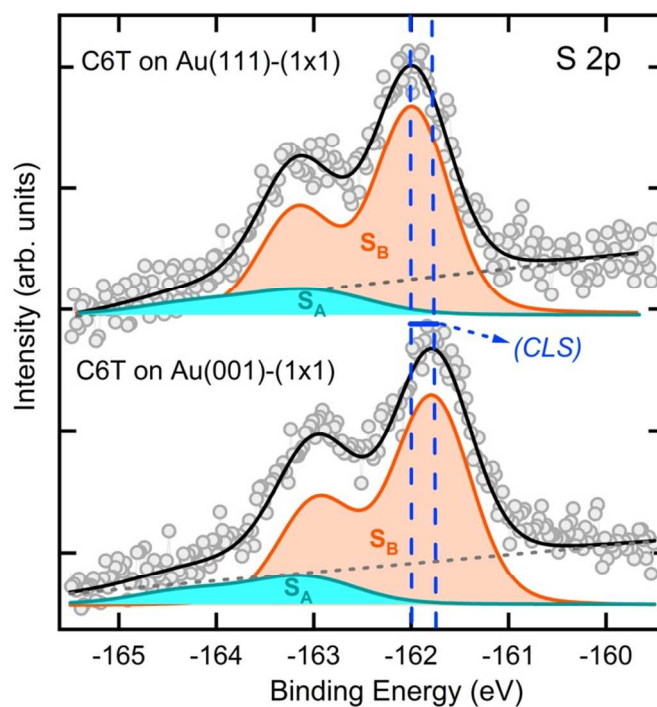


**Figure 1.** Comparison of S 2p XPS spectra for C6T SAMs on Au(111)-(1 × 1) and Au(001)-(1 × 1) obtained after a incubation of 24 h in a 100 μM ethanolic solution. Best fits (black line), S<sub>A</sub>: physisorbed molecules (free R-SH, disulfide (S-S bonds) or dialkyl sulfide species, S<sub>B</sub>: chemisorbed thiolate (R-S-Au bonds). The Core Level Shift (CLS) is shown in the figure.

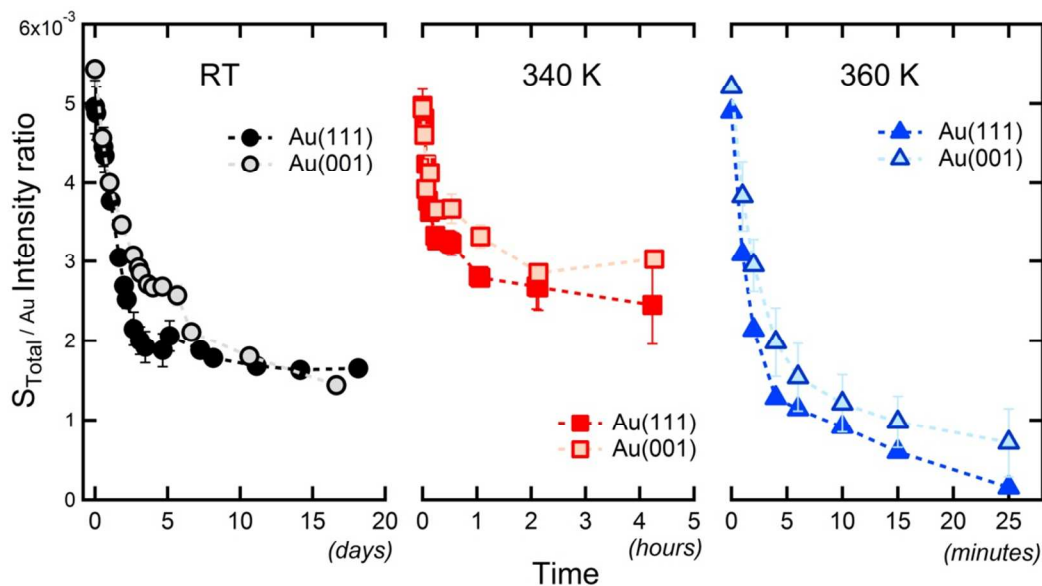


**Figure 2:**  $S_{\text{Total}}/\text{Au}$  intensity ratio as a function of annealing time at RT (days), 340 K (hours) and 360 K (min) in UHV conditions for hexanethiol SAMs on the Au(111)-(1 × 1) (full symbols) and Au(001)-(1 × 1) surfaces (open symbols).

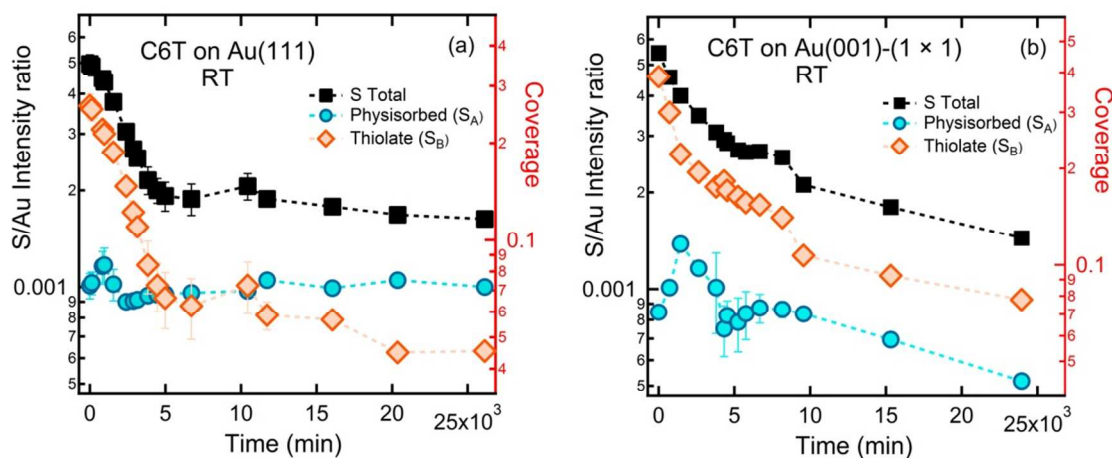


**Figure 3:**  $S_{\text{Total}}/\text{Au}$ ,  $S_{A(\text{physisorbed})}/\text{Au}$  and  $S_{B(\text{thiolate})}/\text{Au}$  intensity ratio as a function of storage time in UHV conditions at RT for hexanethiol SAMs on the preferred oriented Au(111)-(1 × 1) polycrystalline substrate (a) and Au(001)-(1 × 1) single-crystal surfaces (b).

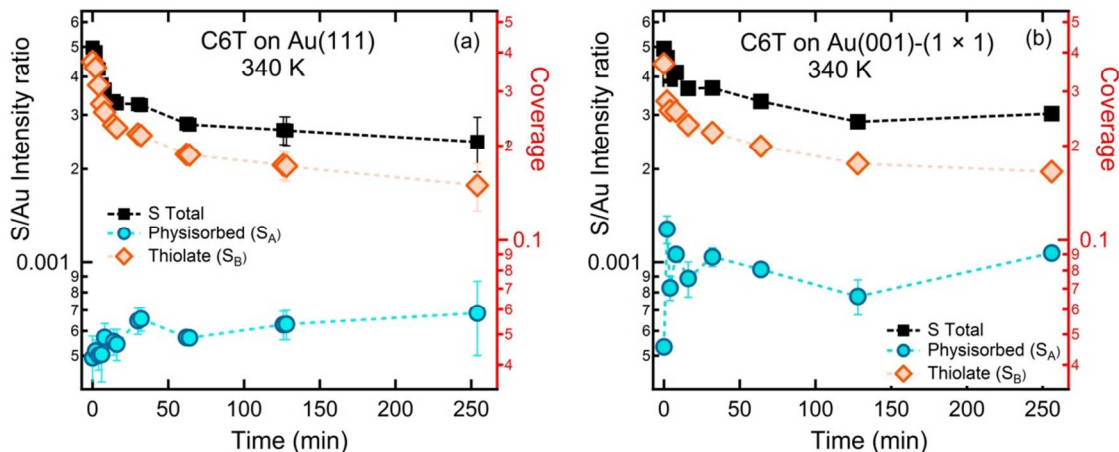


**Figure 4:**  $S_{\text{Total}}/\text{Au}$ ,  $S_{A(\text{Physisorbed})}/\text{Au}$  and  $S_{B(\text{thiolate})}/\text{Au}$  intensity ratio as a function of annealing time at 340 K in UHV conditions for C6T monolayers on the Au(111) (a) and Au(001)-(1 × 1) (b) single-crystals surfaces.

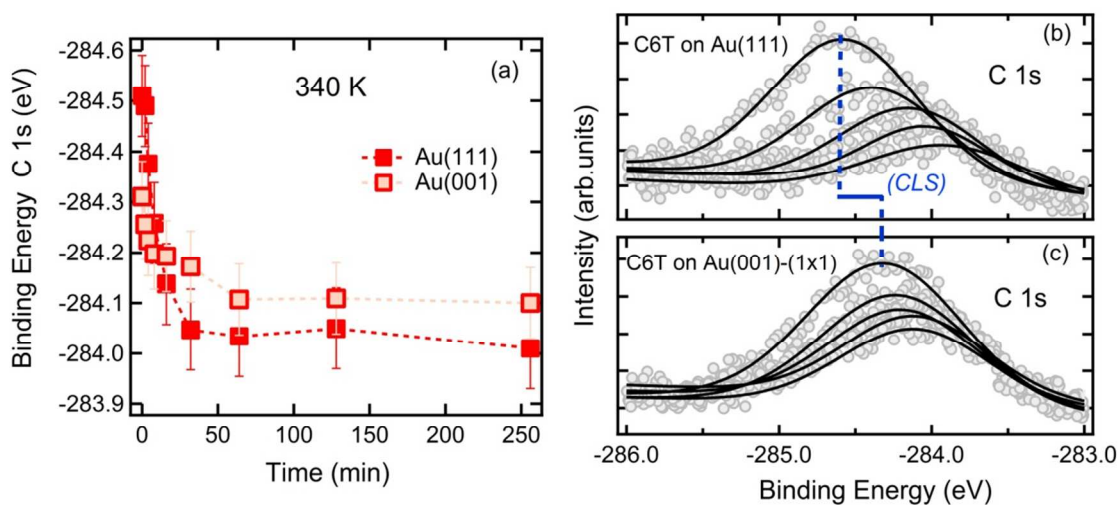


**Figure 5.** (a) BE of C 1s peak as a function of annealing time at 340 K in UHV conditions for hexanethiol SAMs on the Au(111)-(1 × 1) (full symbols) and Au(001)-(1 × 1) surfaces (open symbols). (b) Comparison of C 1s XPS spectra for C6T SAMs on Au(111) and (c) Au(001) obtained after a incubation of 24 h in a 100  $\mu\text{M}$  ethanolic solution and in the course of the thermal desorption to 340 K. Also shown the best fit spectra as a solid black line.

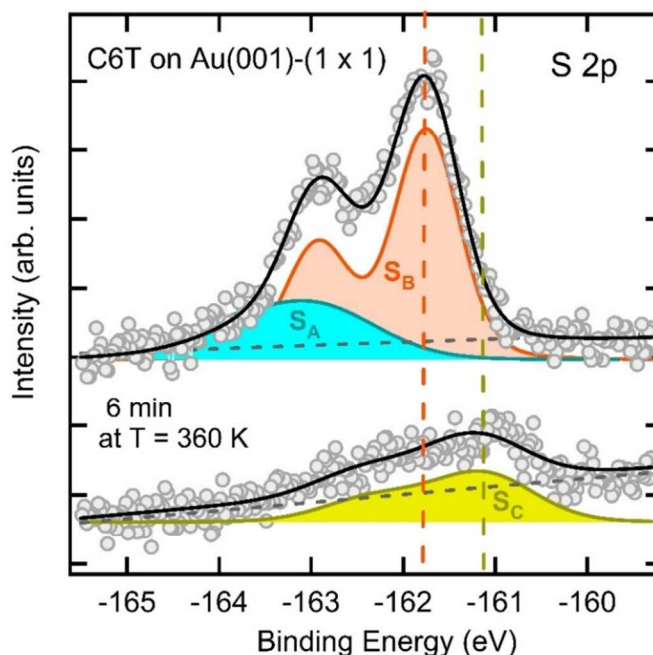


**Figure 6:** S 2p XPS spectra for the C6T SAM on Au(001)-(1×1) single-crystal obtained after a 24 h incubation and after annealing the sample 6 minutes at 360 K. Best fits (black line),  $S_A$ : physisorbed molecules (free R-SH, disulfide species (S–S bonds) or dialkylsulfide),  $S_B$ : chemisorbed thiolate,  $S_C$ : adsorbed sulfur when the C-S bond is broken.

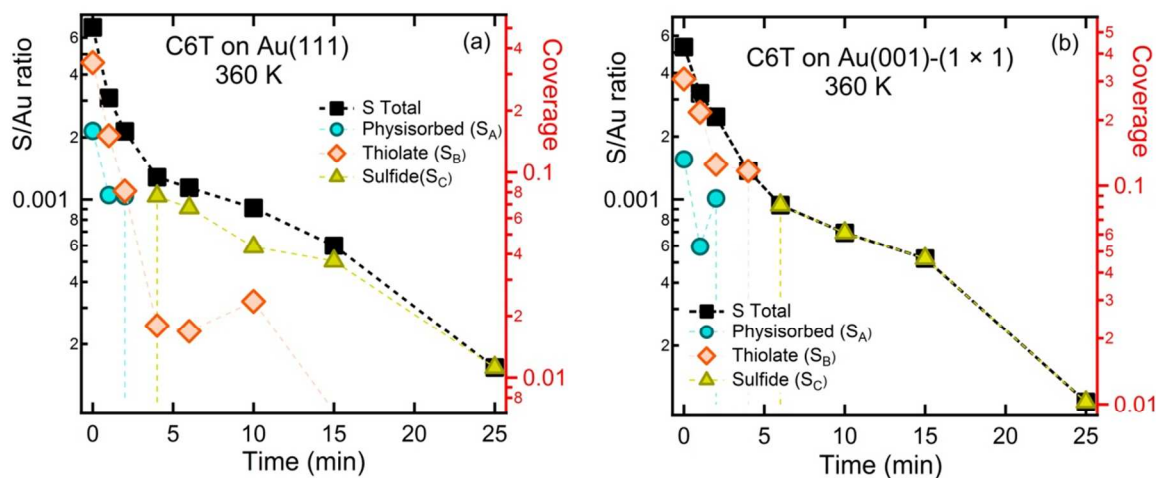


**Figure 7:**  $S_{\text{Total}}/\text{Au}$ ,  $S_{A(\text{physisorbed})}/\text{Au}$ ,  $S_{B(\text{thiolate})}/\text{Au}$  and  $S_{C(\text{sulfide})}/\text{Au}$  intensity ratio as a function of annealing time at 360 K in UHV conditions for C6T monolayers on the Au(111)-(1 × 1) (a) and Au(001)-(1 × 1) surfaces (b).

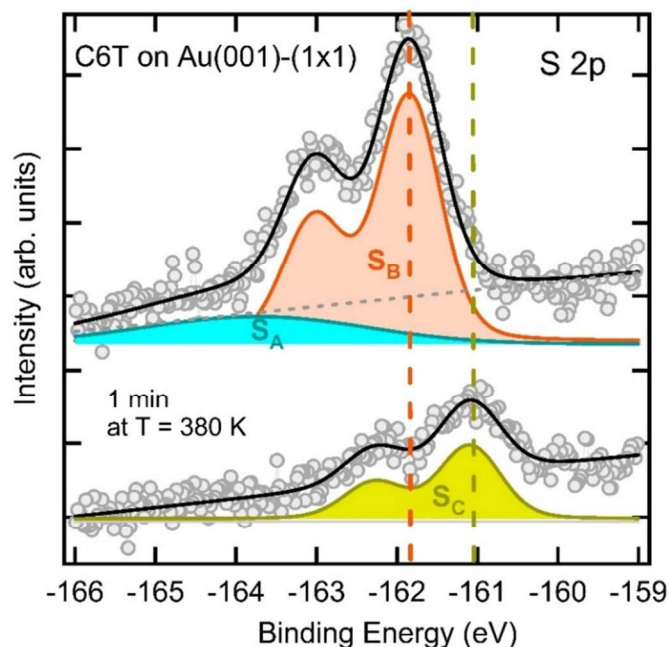


**Figure 8:** S 2p XPS spectra for the C6T SAM on Au(001)-(1 × 1) obtained after a 24 h incubation and after annealing the sample 1 minutes at T = 380 K. Best fits (black line), S<sub>A</sub>: physisorbed molecules (free R-SH, disulfide species (S-S bonds) or dialkylsulfide), S<sub>B</sub>: chemisorbed thiolate, S<sub>C</sub>: adsorbed sulfur when the C-S bond is broken.

## TOC Graphic

